The circadian clock gene circuit controls protein and phosphoprotein rhythms in Arabidopsis thaliana

The Circadian Clock Gene Circuit Controls Protein and Phosphoprotein Rhythms in *Arabidopsis thaliana*

Authors

Johanna Krahmer, Matthew Hindle, Laura K. Perby, Helle K. Mogensen, Tom H. Nielsen, Karen J. Halliday, Gerben van Ooijen, Thierry Le Bihan, and Andrew J. Millar

Correspondence

johanna.krahmer@unil.ch;
Andrew.Millar@ed.ac.uk

Graphical Abstract

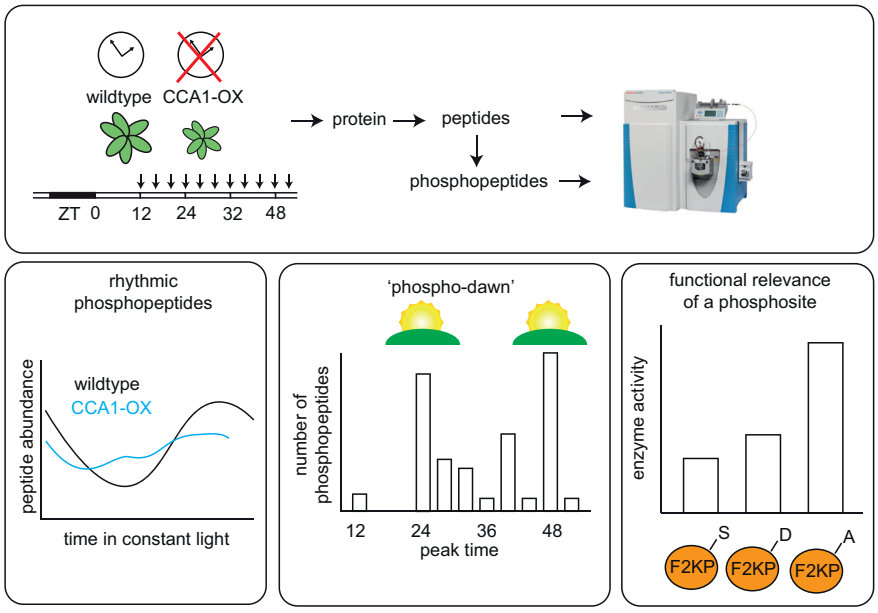

In Brief

Plants have circadian rhythms, driven by a transcription factor network. Circadian clock research has therefore focused on transcriptional regulation. However, nontranscriptional processes also play a role. Therefore, we here present circadian (phospho)proteomics time courses. We find rhythmically phosphorylated proteins with diverse biological roles and demonstrate functional relevance of one example. Most of these rhythms require the transcriptional oscillator. Moreover, most rhythmic phosphorylations peak around dawn, which is a focus of our analysis. These results increase our knowledge of nontranscriptional circadian processes.

Highlights

- Circadian (phospho)proteomics time courses of plants with or without functional clock.
- Most protein abundance/phosphorylation rhythms require a transcriptional oscillator.
- The majority of rhythmic phosphosites peak around subjective dawn ("phospho-dawn").
- A phosphorylated serine of the metabolic enzyme F2KP has functional relevance.

2022, Mol Cell Proteomics *21(1)*, 100172

https://doi.org/10.1016/j.mcpro.2021.100172

The Circadian Clock Gene Circuit Controls Protein and Phosphoprotein Rhythms in *Arabidopsis thaliana*

Johanna Krahmer[1,2,*], Matthew Hindle[3], Laura K. Perby[4], Helle K. Mogensen[4], Tom H. Nielsen[4], Karen J. Halliday[2], Gerben van Ooijen[2], Thierry Le Bihan[1], and Andrew J. Millar[1,*]

Twenty-four-hour, circadian rhythms control many eukaryotic mRNA levels, whereas the levels of their more stable proteins are not expected to reflect the RNA rhythms, emphasizing the need to test the circadian regulation of protein abundance and modification. Here we present circadian proteomic and phosphoproteomic time series from *Arabidopsis thaliana* plants under constant light conditions, estimating that just 0.4% of quantified proteins but a much larger proportion of quantified phospho-sites were rhythmic. Approximately half of the rhythmic phospho-sites were most phosphorylated at subjective dawn, a pattern we term the "phospho-dawn." Members of the SnRK/CDPK family of protein kinases are candidate regulators. A *CCA1*-overexpressing line that disables the clock gene circuit lacked most circadian protein phosphorylation. However, the few phospho-sites that fluctuated despite *CCA1*-overexpression still tended to peak in abundance close to subjective dawn, suggesting that the canonical clock mechanism is necessary for most but perhaps not all protein phosphorylation rhythms. To test the potential functional relevance of our datasets, we conducted phosphomimetic experiments using the bifunctional enzyme fructose-6-phosphate-2-kinase/phosphatase (F2KP), as an example. The rhythmic phosphorylation of diverse protein targets is controlled by the clock gene circuit, implicating posttranslational mechanisms in the transmission of circadian timing information in plants.

Most circadian observations in the well-characterized plant species *Arabidopsis thaliana* can be explained by a genetic network of mostly negatively interacting transcription factors (1, 2). In addition to transcriptional interactions, this transcriptional-translational feedback loop (TTFL) system requires posttranslational modification of transcription factor proteins (3). Phosphorylation of CCA1 by casein kinase (CK) 2, for example, is necessary for the circadian clock function (4).

Protein phosphorylation is involved in the circadian clock mechanism not only in plants but also in fungi, animals, and cyanobacteria (3, 5). While the transcription factors of TTFLs in animals, fungi, and plants are not evolutionarily conserved (3), many kinases that play a role in circadian timekeeping are similar across eukaryotes. For instance, CK2 is also important for circadian timing in mammals (6) and fungi (7). Protein phosphorylation is also involved in the output of the circadian clock (8). However, only one study has so far addressed the question of how pervasive circadian protein phosphorylation is in higher plants (9).

In circadian biology, transcriptional studies have long dominated research efforts, leading to the well-established TTFL models (*e.g.*, (1, 2, 10–12)). However, it has become apparent that protein abundance and posttranslational modification cannot be ignored, since these do not simply follow transcript expression patterns (*e.g.*, (13–15)). There is even evidence that circadian oscillations can be driven by non-transcriptional oscillators (NTOs) that are independent of rhythmic transcription. The cyanobacterial circadian clock is based on rhythmic autophosphorylation of the KaiC protein together with the KaiA and KaiB proteins, and this mechanism does not even require a living cell to create oscillations (16). Evidence for NTOs also exists in eukaryotes; the protein peroxiredoxin (PRX) is rhythmically overoxidized in the absence of transcription in algae and human red blood cells (17, 18). Circadian rhythms of PRX overoxidation were also observed in organisms that have impaired circadian oscillators, in mutants of the fungus *Neurospora crassa* and in transgenic Arabidopsis plants (19). The circadian PRX overoxidation rhythm even exists in cyanobacteria and archaea

From the [1]SynthSys and [2]Institute for Molecular Plant Science, School of Biological Sciences, University of Edinburgh, Edinburgh, United Kingdom; [3]The Roslin Institute, Royal (Dick) School of Veterinary Studies, Edinburgh, United Kingdom; [4]Section for Molecular Plant Biology, Department of Plant and Environmental Sciences, University of Copenhagen, Copenhagen, Denmark

*For correspondence: Johanna Krahmer, johanna.krahmer@unil.ch; Andrew J. Millar, Andrew.Millar@ed.ac.uk.

Present address for Johanna Krahmer: Center for Integrative Genomics, Faculty of Biology and Medicine, University of Lausanne, Lausanne, Switzerland.

https://doi.org/10.1016/j.mcpro.2021.100172

(19). In addition, circadian magnesium and potassium ion transport has been observed across eukaryotes and can occur in transcriptionally inactive *Ostreococcus tauri* and human red blood cells (20, 21). Therefore, at least some eukaryotes possess NTOs that appear to be evolutionarily ancient and conserved (3).

With mass spectrometer technology becoming more and more advanced, several circadian proteomics studies have been conducted in different species, such as proteomics analyses of protein abundance time courses (15, 22–25), proteomics specifically at the day/night transition (25, 26), or circadian phosphoproteomics (9, 24).

In this study, we used mass-spectrometry-based proteomics and phosphoproteomics on circadian time courses to address the following questions: (1) How pervasive are rhythms in protein abundance and phosphorylation as a clock output in a normally functioning circadian clock system, and what are the characteristics of such rhythms? and (2) Can protein abundance or phosphorylation be rhythmic in a plant with a disabled transcriptional oscillator? To investigate (1), we used a time course of WT plants, and for addressing (2), we generated time courses from plants overexpressing the *CIRCADIAN CLOCK-ASSOCIATED 1* gene (CCA1-OX), which have an impaired TTFL (27). We generated global proteomics and phosphoproteomics data in parallel from the same protein extracts. Our analysis revealed that the transcriptional oscillator is required for most rhythmic protein phosphorylation, and that most rhythmic phosphopeptides peak at subjective dawn. We also found this "phospho-dawn" trend among the time courses of fluctuating phosphopeptides in the CCA1-OX. Finally, we selected a phosphosite of the bifunctional enzyme fructose-6-phosphate-2-kinase/fructose-2,6-bisphosphatase (F2KP) to illustrate how our data can be used to study the mechanisms of clock output pathways that connect to central carbon metabolism.

EXPERIMENTAL PROCEDURES

Plant Material

A. thaliana WT (Col-0 accession) and a *CCA1* over-expressing plants ("CCA1-OX," (27)) were used in this study. Seeds were germinated and grown on plates (2.15 g/l Murashige & Skoog medium Basal Salt Mixture (Duchefa Biochemie), pH 5.8 (adjusted with KOH), and 12 g/l agar (Sigma)) at 85 μmol m^{-2} s^{-1} white fluorescent lights at 21 °C in Percival incubators for 11 days in 12 h light, 12 h dark cycles. Seedlings were transferred to soil and grown for 11 more days at a light intensity of 110 μmol m^{-2} s^{-1} in the same light–dark cycle.

Experimental Design and Statistical Rationale

After plants had grown for a total of 22 days, from ZT 0 of day 23 lights remained switched on continuously and collection of plant material started at ZT 12 (dataset I) or ZT 24 (dataset II). In dataset I, six time points at 4 h intervals were taken with five replicates for each time point, harvesting eight rosettes for the WT and 12 rosettes for the CCA1-OX. In dataset II, also at 4 h intervals, at least six replicates of eight rosettes each were taken for the WT, five (16 rosettes each) of the CCA1-OX. In dataset I, the time course was therefore sampled from ZT12 to ZT32, in dataset II from ZT24 to 48 (CCA1-OX) or ZT24 to ZT52 (WT).

Our rationale for starting the time courses at either ZT12 or ZT24 rather than a later time point was to enhance rhythm detection by reducing desynchronization that is expected after longer periods of time (28) from the typically relatively small amplitudes and higher technical variability of proteomics compared with transcript analysis (29).

Statistical analysis of time courses required assessment of not only changes but also rhythmicity. We therefore used both analysis of variance (ANOVA) and JTK_CYCLE as statistical tools (see below for details).

Sample Preparation

Rosettes without roots were harvested by flash-freezing in liquid nitrogen. Protein extraction and precipitation were carried out according to method "IGEPAL-TCA" described by (30). Briefly, protein was extracted and precipitated with TCA and phase separation, then washed with methanol and acetone. In total, 500 μg resuspended protein was digested using a standard in-solution protocol and peptides were desalted. Before drying, eluted peptides were separated into two parts: 490 μg of the digest was used for phosphopeptide enrichment, 10 μg was saved for global protein analysis. Phosphopeptides were enriched using the Titansphere spin tip kit (GL Sciences Inc) and desalted on BondElut Omix tips (Agilent) according to the manufacturers' instructions.

Mass Spectrometry, Peptide Merging, and Progenesis Analysis

LC-MS/MS measurement and subsequent analysis were carried out as previously described (30): Dried peptides were dissolved in 12 μl (phosphoproteomics) or 20 μl (global proteomics) 0.05% TFA and passed through Millex-LH 0.45 μm (Millipore) filters. In total, 8 μl was run on an on-line capillary- HPLC-MSMS system consisting of a micropump (1200 binary HPLC system, Agilent) coupled to a hybrid LTQ-Orbitrap XL instrument (Thermo-Fisher). Reverse-phase buffer used for LC-MS separation was buffer A (2.5% acetonitrile, 0.1% FA in H_2O) and buffer B (10% H_2O, 90% acetonitrile, 0.1% formic acid, 0.025% TFA). LC peptide separation was carried out on an initial 80 min long linear gradient from 0% to 35% buffer B, then a steeper gradient up to 98% buffer B over a period of 20 min, then remaining constant at 98% buffer B for 15 min until a quick drop to 0% buffer B before the end of the run at 120 min. Peak lists were generated with the Progenesis software (version 4.1.4924.40586).

The tair Arabidopsis_1rep (version 20110103, 27,416 protein entries) database was used for data-dependent detection, using the Mascot search engine (version 2.4), including all peptide sequences of rank smaller than 5. Search parameters were as follows: charges 2+, 3+ and 4+, trypsin as enzyme, allowing up to two missed cleavages, carbamidomethyl (C) as a fixed modification, Oxidation (M), Phospho (ST) and Phospho (Y), Acetyl(Protein N-term) as variable modifications, a peptide tolerance of 7 ppm, and MS/MS tolerance of 0.4 Da, peptide charges 2+, 3+, and 4+, on an ESI-trap instrument, with decoy search and an ion cutoff of 20. In all but one cases, these parameters resulted in a false-discovery rate (FDR), of less than 5% with one exception (phosphoproteomics dataset I: 3.5%, phosphoproteomics dataset II: 3.2, global dataset I: 6.8%, global dataset II: 4.5%, calculated using the formula 2*d/(n+d) (31), n and d being the number of hits in the normal and decoy databases, respectively, using an ion score cutoff of 20). Peptides were quantified by their peak area by Progenesis, and proteins were quantified by using the sum of the quantitation of all unique peptides. Where peptides matched very similar proteins,

multiple accession numbers are shown in exported results from Progenesis (supplemental Data S1 and S2; Table 2).

In order to remove duplicates of phosphopeptides due to alternative modifications other than phosphorylation or missed cleavages, we used the qpMerge software following the Progenesis analysis (32). The data are publicly available in the pep2pro database (33) at http://fgcz-pep2pro.uzh.ch (Assembly names "ed.ac.uk Global I," "ed.ac.uk Global II," "ed.ac.uk Phospho I," "ed.ac.uk Phospho II") and have been deposited to the ProteomeXchange Consortium (http://proteomecentral.proteomexchange.org) *via* the PRIDE partner repository (34) with the dataset identifier PXD009230. Exported.csv files from Progenesis with all peptide and protein quantifications can be found in the online supplemental data (supplemental Data S1 and S2).

General Statistics and Outlier Removal

Results of statistical analyses are summarized in supplemental Data S3. Outlier analysis, statistics, and Venn diagrams were done using R version 3.2.1 (http://www.r-project.org/). Zero values for the quantification were exchanged for "NA." For outlier analysis and parametric tests such as ANOVA, arcsinh transformed data were used to obtain a normal distribution, while untransformed data were used for plotting time courses and for the nonparametric JTK_CYCLE analysis. For phosphoproteomics analysis all replicates in which the Pearson correlation coefficient among replicates of the same time point was lower than 0.8 were regarded as outliers (supplemental methods, supplemental Data S4). In global dataset II, the first run replicate of each time point had to be excluded as an outlier due to an apparent drift (supplemental Data S4). To generate heat maps, the abundance of each peptide or protein was normalized by the time course mean of the peptide or protein, followed by taking the log2 to center values around 0, and the heatmap.2 function from the pvclust R package was applied (http://cran.r-project.org/package=pvclust) (35).

JTK_CYCLE Analysis

We used the R-based tool JTK_CYCLE (36) to determine rhythmicity, with the following modifications: (1) we ran the JTK_CYCLE algorithm for each phosphosite or protein separately rather than the entire list, to allow handling of missing quantification values for some replicates. Benjamini–Hochberg (BH) (37) correction of p-values was carried out after application of the JTK_CYCLE tool. (2) Since our time course durations are close to the periods of rhythms we are searching for, some identifications were assessed as rhythmic by the original JTK_CYCLE tool that were increasing or decreasing continually over the entire time course. We excluded these from the group of rhythmic identifications ("excl." in p-value column in supplemental Data S3 and S5). For dataset-wide analyses we used $p < 0.05$ as a cutoff for rhythmicity and then trusted results that agree between experiments. Similarly, for judging individual time courses, we focus on those with $p < 0.05$ in both datasets.

Kinase Prediction Using GPS3.0

Kinases for each site were predicted using the *A. thaliana* specific GPS 3.0 prediction tool in its species-specific mode for *A. thaliana* (http://gps.biocuckoo.cn/download.php) (38). For each phosphorylation site, an amino acid sequence was generated that contained 50 amino acids on either side of the phosphorylated residue using a python script. This resulted in 101 amino acid long sequences, unless the phosphosite was closer than 50 residues to the C or T terminus in which case the missing positions were filled by "X." The phosphopeptides used as foreground were the significantly rhythmic phosphosites (JTK_CYCLE p-value < 0.05) peaking at a given time point, all other phosphosites identified in the same experiment were used as background. The high threshold setting was used to minimize false-positive predictions and searches were done for S and T residues. In order to reduce the complexity of the dataset, we used a simplification: where kinases from different families were predicted, only the one with the highest difference between score and cutoff was used. For foreground and background, the numbers of predictions for each occurring kinase group were counted and the Fisher's exact test was used to determine predicted kinases that were significantly enriched in the foreground group ($p < 0.05$).

GO Analysis

For GO analysis, foreground and background were chosen as in the kinase prediction analysis. With these groups, GO analysis was conducted using the topGO script (39), followed by Fisher's exact test to determine enrichment of terms (supplemental Data S6).

Generation of F2KP Point Mutations and Expression Constructs

The F2KP coding sequence in the pDONR221 vector, lacking a stop codon, was kindly provided by Dr Sebastian Streb, ETH Zürich. The QuikChange Lightning Site-Directed Mutagenesis kit (Agilent Technologies) was used to introduce point mutations using primer pair AspF and AspR for mutation of S276 to aspartic acid or AlaF and AlaR for mutation to alanine (supplemental Table S1). The WT or mutated F2KP coding sequences were amplified by PCR using primers F2KP-F and F2KP-R (supplemental Table S1), introducing restriction sites for AflII (3′ end) and XbaI (5′ end) and a stop codon. Using these restriction sites, digested PCR products were ligated into the pmcnEAVNG expression vector, which allows expression in *E.coli* with an N-terminal GST tag and a T7 promoter for IPTG inducibility. Plasmids were transformed into Rosetta2(DE3)pLysS Competent expression strain (Novagen).

Expression of GST-F2KP Constructs in E. coli *Cells*

The three constructs, WT, S276D, and S276A, were expressed in *E. coli* and purified using the GST tag. Two independent expression experiments were performed (experiment 1 and experiment 2), each in triplicates. In total, 200 ml *E. coli* cultures were grown at 37 °C with 100 μg/ml ampicillin and 25 μg/ml chloramphenicol and induced with 1 mM IPTG at OD_{600} values between 0.6 and 0.8. Cells were harvested by centrifugation after 2.5 h of expression at 37 °C. Each pellet was from 50 ml bacterial culture. For purification of GST-F2KP, pellets were lysed in 2.5 ml PBS with Complete protease inhibitor cocktail (Roche) with a probe sonicator. After clearing of the lysates, AP was carried out using GSH-agarose beads, with 167 μl GSH-agarose bead suspension (Protino glutathione agarose 4B, Macherey-Nagel), a binding incubation of 30 min at room temperature, four washes with 10× the volume of the bead suspension and elution in PBS with 100 mM reduced glutathione (pH 8.0) three times 30 min at room temperature.

F2KP Activity Assay

F2KP activity of purified F2KP was measured as described in (40) (F-2,6-BP producing reaction) and (41) (measurement of generated F-2,6-BP by its activation of PFP and subsequent production of NADH produced from glycolytic enzymes).

Western Blot Quantification of F2KP Concentration in AP Eluates

To test whether the differences in F2KP activity of eluates could be caused by differences in abundance in the eluate, we quantified the amount of F2KP in equal volumes of eluates by western blotting. Samples were prepared for SDS-PAGE with 25% 4xLDS (Life Technologies, NP0008) and 20 mM DTT and were incubated at 70 °C for 10 min. Two concentration series of an equal mix of all three eluates were loaded on each gel for relative quantitation. Individual eluates

were examined in duplicates (expression 1) or triplicates (expression 2). In total, 4–12% Bis-Tris Gels (Life Technologies) were run and protein was blotted onto nitrocellulose membrane using the iBlot system. Two primary antibodies were used in parallel: anti-F2KP from rabbit, raised against amino acids 566–651 (42) and anti-GST from mouse (Thermo Scientific), both at a dilution of 1:1000 overnight. Secondary antibodies were goat-anti-rabbit (IRDye800CW, LI-COR) and goat-anti-mouse (IRDye680RD, LI-COR). Bands were quantified using the ImageStudioLite (version 2) software.

RESULTS

Circadian Protein Phosphorylation Requires the Canonical Transcriptional Oscillator

We generated global proteomics and phosphoproteomics datasets for two independent circadian time courses and for two genotypes each—WT and the CCA1-OX line, which has an impaired circadian oscillator (27). This resulted in four datasets: global protein and phosphopeptide datasets I (Zeitgeber time (ZT) 12 to ZT32) and datasets II (ZT24 to ZT48 (CCA1-OX) or ZT52 (WT)) (Fig. 1, *A* and *B*). We removed outliers before conducting further statistical analysis (supplemental Data S4).

We identified 2287 phosphopeptides in dataset I, 1664 in dataset II, which condensed to between 1000 and 1500 in each dataset after applying qpMerge (32) to remove duplicate phosphopeptides (Table 1*A*). These were from several hundred proteins in each dataset and over 1000 in both datasets together (Table 1*B*). In the global protein analysis, we identified 1896 and 1340 proteins in dataset I and II, respectively, adding up to a total of 2501 for both datasets combined (Table 1, *A* and *B*). To assess the circadian rhythmicity of each phosphopeptide or protein, we employed the nonparametric JTK_CYCLE method (36) as it can be applied to time courses of only one cycle, taking the curve shape into account. Unless otherwise stated, we considered periods of 22–26 h and excluded continuously increasing or decreasing profiles from the group of rhythmic phosphopeptides or proteins. In dataset

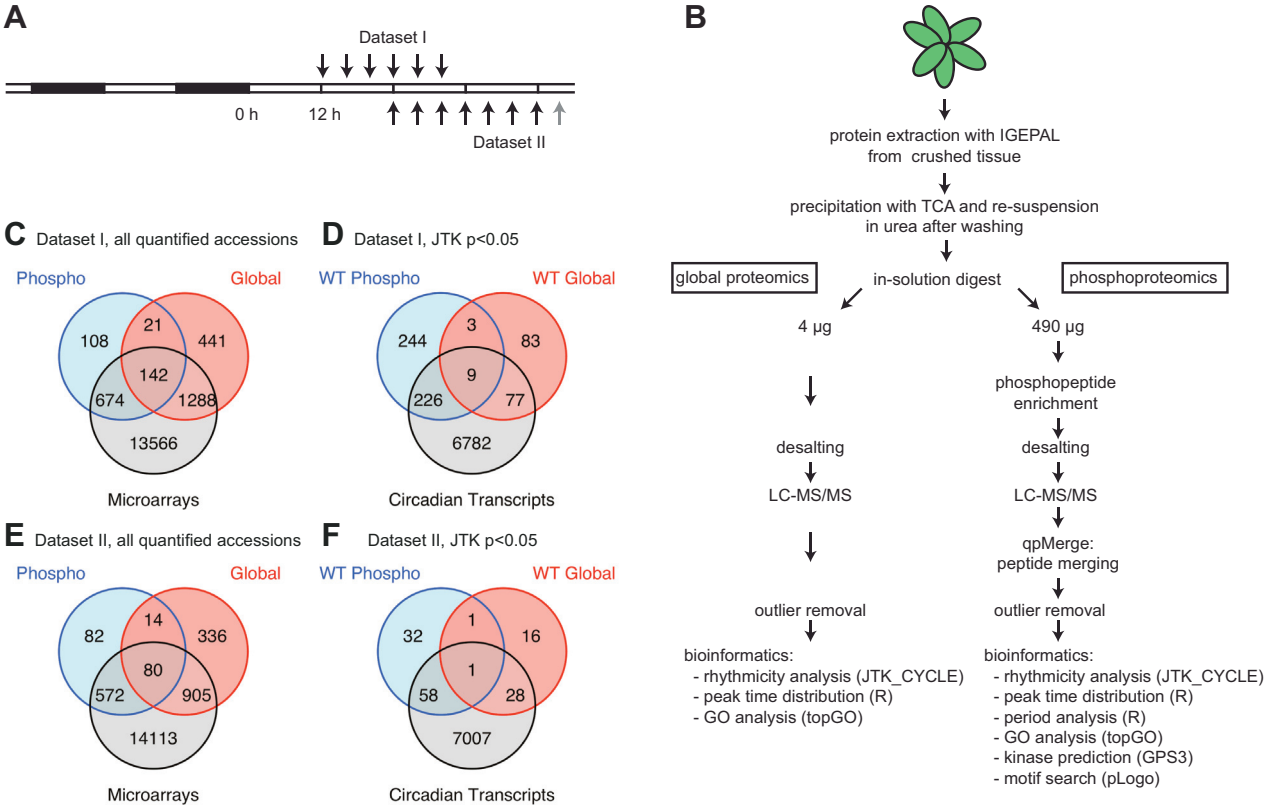

FIG. 1. **Experiment workflow and comparison of protein and phosphopeptide numbers with published transcriptome time courses.** *A*, WT and CCA1-OX plants were grown in 12 h light:12 h dark cycles for 22 days and then subjected to continuous light. In dataset I, rosettes were harvested every 4 h from ZT12, in dataset II from ZT24 until ZT48 (*black arrows*) with an additional WT time point at ZT52 (*gray arrow*). *B*, sample processing and data analysis workflow: Plants were crushed and protein was extracted, precipitated, and digested in-solution. Peptides were split into 10 µg for global protein analysis (of which 4 µg were injected) and 490 µg for phosphopeptide enrichment on TiO_2 spin tips. Peptides were analyzed by LC-MS/MS. Outliers were removed before further bioinformatics analysis. *C*, Venn diagrams showing overlap of quantified (*C* and *E*) and rhythmic (WT only; *D* and *F*) transcripts (51), proteins and phosphoproteins in dataset I (*C* and *D*) and dataset II (*E* and *F*).

TABLE 1
Identification counts for global and phosphoproteomics datasets

A	Dataset I				Dataset II			
Numbers of quantified and changing identifications in each dataset	Global proteomics		Phosphoproteomics		Global proteomics		Phosphoproteomics	
	WT	CCA1-OX	WT	CCA1-OX	WT	CCA1-OX	WT	CCA1-OX
Quantifiable identifications before merging	1896 proteins		2287 phosphopeptides		1340 proteins		1664 phosphopeptides	
Quantifiable identifications after merging			1498 from 944 proteins				1132 from 747 proteins	
Significantly changing (ANOVA $p < 0.05$)	245	147	406	296	68	46	88	83
Adjusted for multiple testing (ANOVA $q < 0.05$)	13	3	56	4	3	2	14	7
Rhythmic by JTK_CYCLE ($p < 0.05$)	171	122	606 from 481 proteins	37 from 32 proteins	45	57	100 from 91 proteins	17 from 17 proteins
Adjusted for multiple testing (JTK:CYCLE $q < 0.05$)	6	0	338	2	6	0	26	0
JTK_CYCLE $p < 0.05$ in both genotypes	17		22		9		3	

B	Global proteomics		Phosphoproteomics	
Shared and added numbers of both datasets	WT	CCA1-OX	WT	CCA1-OX
JTK $p < 0.05$ detected in both datasets	8	4	48	2
All quantified protein IDs detected in both datasets	137		626	
Sum of all quantifiable protein IDs in both datasets	2501		1065	

Protein IDs of peptides are used for simplicity of comparison.

I, 606 (40%) phosphopeptides were rhythmic in the WT, in dataset II 100 (8.8%) based on the *p*-value of the individual timeseries. In total, 338 (23%) (dataset I) and 26 (2.3%) (dataset II) were rhythmic after adjusting for multiple testing ("*q*-value" < 0.05) (37). The fraction of rhythmic proteins in the global proteomics analysis was smaller than in the case of phosphopeptides: 171 (9.0%) in dataset I, 45 (3.4%) in dataset II had JTK_CYCLE *p*-values < 0.05. Six proteins also had *q*-values < 0.05 in each dataset (0.32% in dataset I, 0.45% in dataset II). Phosphopeptides and proteins with JTK_CYCLE *p* < 0.05 in both datasets are listed in Table 2.

In the CCA1-OX line, 37 (2.5%) phosphopeptides had a JTK_CYCLE *p*-value < 0.05 in dataset I, 17 (1.5%) in dataset II; in the global datasets, 122(6.4%) and 57 (4.3%) had a JTK_CYCLE *p*-value < 0.05 in datasets I and II, respectively. After adjusting for multiple testing, only two significant identifications remained for the CCA1-OX phosphopeptides in dataset I and none in dataset II (Table 1*A*). This analysis suggests that a functional TTFL is required for most rhythmic protein phosphorylation.

For further whole-dataset analyses, we used JTK_CYCLE *p*-value < 0.05 as a criterion for rhythmicity and treated results as reliable if rhythmic scores were obtained from separate analysis of each dataset. This approach is also supported by comparison with existing data: Among the phosphopeptides with $p < 0.05$ and $q > 0.05$ were phosphosites that were previously shown to be rhythmic with almost identical phases, such as RTT(pS)LPVDAIDS of WITH NO LYSINE (WNK) 1, and TL(pS)STPLALVGAK of CHLORIDE-CHANNEL-A (CLC-A) (supplemental Data S3) (9). As expected, the global proteomic analysis did not quantify all the proteins identified by the phosphoproteomic enrichment (Fig. 1, *C* and *E*). We found very few proteins with rhythms in abundance as well as rhythmic phosphopeptides (12 in dataset I, 2 in dataset II). About half of the rhythmic phosphopeptides or proteins had rhythmic transcripts (Fig. 1, *D* and *F*).

For a more quantitative comparison of the phosphopeptides that were classified as rhythmic in both dataset in the WT, we determined the fold changes between ZT24 and ZT28 and between ZT28 and ZT32 (*i.e.*, the time intervals shared between the two datasets). Regression analysis revealed that the dynamics of both datasets are significantly correlated within these time intervals ($p = 0.0012$ for ZT24 to ZT28 and $p = 3.1 \times 10^{-13}$ for ZT28 to ZT32) (supplemental Fig. S1*A*). Peak phase differences of the same set of shared rhythmic phosphopeptides are centered around 0 h and 20 h, confirming similar dynamics in both datasets (supplemental Fig. S1*B*).

TABLE 2
List of all proteins and phosphopeptides that are rhythmic in WT or CCA1-OX in both datasets

A. Phosphopeptides, WT

Accession	Description	Peptide ID dataset I	Peptide ID dataset II	Peptide sequence	Phospho residue(s)	*p*-value dataset I	*p*-value dataset II	*q*-value dataset I	*q*-value dataset II	Peak dataset I	Peak dataset II
AT4G32340	TPR-like superfam. pr.	15668	12823	SASSLDLNLR	3	9.5E-05	1.9E-09	5.7E-03	2.1E-06	**12**	**32**
AT2G33830	DRM2	6246	2709	TVAAVAGSPGT PTTPGSAR	13/11	2.0E-02	2.0E-08	6.5E-02	8.9E-06	**12**	**40**
AT4G31700	RPS6A	8624	1785	SRLSSAAAKPSVTA	1,4,5	2.0E-06	2.8E-07	4.9E-04	3.9E-05	**24**	**24**
			778	SRLSSAAAKPSVTA	1,4,5/1,4,11	2.0E-06	2.4E-08	4.9E-04	8.9E-06	**24**	**24**
			21	SRLSSAAAKPSVTA	1,4,5/1,4	2.0E-06	9.5E-07	4.9E-04	1.1E-04	**24**	**24**
		2489	3985	LSSAAAKPSVTA	9	1.5E-03	3.6E-03	2.1E-02	1.2E-01	32	48
AT5G10360	RPS6B	41, 1736	28	SRLSSAPAKPVAA	4/1, 4	7.4E-03	4.8E-07	4.0E-02	5.9E-05	32	24
AT3G47470	CAB4	715	636	DLSFTSIGSSAK	3	1.3E-06	1.6E-07	4.9E-04	3.0E-05	**28**	**32**
AT3G07650	COL9	8182	11184	AGEAYDYDPLTPT RSY	15	3.0E-03	2.4E-07	2.7E-02	3.8E-05	24	40
AT5G48250	BBX8	11033	16261	SGEAYDYDPMSPT RSY	15/16	7.4E-03	1.6E-06	4.0E-02	1.6E-04	24	40
AT1G69870	NRT1.7	7142	8476	ISSPGSILDAEK	3	1.7E-04	3.0E-06	6.8E-03	2.8E-04	**24**	**48**
AT5G40890	CLC-A	1783	1852	HRTLSSTPLALVGAK	3, 5	5.1E-05	1.1E-04	4.0E-03	7.3E-03	**24**	**24**
AT5G53420	CCT101.	1950	1997	LGAGLVQSPLDR	8	6.0E-03	1.1E-04	3.6E-02	7.3E-03	**28**	**48**
AT5G20670	DUF1677	4202	5127	TSSSGALPGIDGVESR	3/4	1.9E-03	1.6E-04	2.3E-02	1.0E-02	**28**	**48**
AT1G73980	TTM1	10001	8639	LSLDDDTVSSPK	10	1.7E-02	1.9E-04	5.9E-02	1.1E-02	**28**	**24**
AT1G78020	FLZ6	10297, 1700	3249, 1093	LLSMVTPR	3	1.3E-05	2.1E-04	1.5E-03	1.2E-02	**24**	**24**
		2081, 5542, 5542	2113, 737, 2081	RHSGDFSDAGHFLR	3	2.4E-02	1.5E-03	7.4E-02	6.2E-02	**24**	**24**
AT1G11310	MLO2	1496	3909	SVENYPSSPSPR	7/8, 10	2.3E-04	1.9E-03	7.7E-03	6.9E-02	32	24
AT2G32240	PICC	5883	7383	DIDLSFSSPTKR	8	1.1E-02	4.0E-03	4.9E-02	1.3E-01	**24**	**48**
AT3G13290	VCR	4140	6826	TLSYPTPPLNPQSPR	13	3.0E-03	5.4E-03	2.7E-02	1.6E-01	**28**	**48**
AT4G35100	PIP3A	140	214	ALGSFRSNATN	4, 7	1.1E-02	8.0E-03	4.9E-02	1.9E-01	**28**	**24**
AT5G38640	NagB/RpiA/CoA transferase-like superfam. pr.	4683	1690	DFPDGSTTASPGR	10	6.0E-03	8.8E-03	3.6E-02	2.0E-01	32	24
AT1G37130	NIA2	4382	2045, 2045	VHDDDEDVSSEDE NETHNSNAVYYK	9, 10	9.0E-04	8.8E-03	1.7E-02	2.0E-01	**28**	**28**
AT3G13530	MAPKKK7	3515	6312	SKLPLVGVSSFR	10	3.0E-03	8.8E-03	2.7E-02	2.0E-01	28	40
AT1G35580	CINV1	903	1066	SVLDTPLSSAR	5, 8	1.7E-02	9.7E-03	5.9E-02	2.1E-01	**24**	**24**
AT1G74780	Major Facilitator Superfam. pr.	6279	4702, 5728	TVPHDYSPLISSPK	12	3.0E-03	9.7E-03	2.7E-02	2.1E-01	**28**	**48**
AT3G27700	zinc finger fam. pr.	**9563**	9073	LDTASDSGAAIASPK	13	4.8E-03	1.1E-02	3.4E-02	2.2E-01	**28**	**48**
AT5G65010	ASN2	**4975**	4842	AGSDLVDPLPK	3	6.9E-04	1.3E-02	1.6E-02	2.4E-01	**28**	**24**
AT4G31160	DCAF1, DDB1-CUL4 associated factor 1	**8754**	7154, 8583	VHEGAPDTEVLL ASPR	14	3.5E-02	1.3E-02	9.3E-02	2.4E-01	**28**	**48**
AT4G13510	AMT1;1	214	110	SPSPSGANTTPTPV	1	3.5E-02	1.4E-02	9.3E-02	2.5E-01	32	48
AT5G23660	SWEET12	14806	17187	LGTLTSPEPVAITVVR	6	9.1E-03	1.8E-02	4.3E-02	3.0E-01	24	40
AT3G26730	RING/U-box superfam. pr.	5794	6017	NQTQSLSPPDVSR	7	1.3E-04	2.2E-02	6.2E-03	3.5E-01	**24**	**24**
AT4G20910	HEN1	15648	13859, 13859	SSSPNVFAAPPILQK	3/2, 3	9.5E-05	2.6E-02	5.7E-03	3.7E-01	**28**	**24**

TABLE 2—*Continued*

A. Phosphopeptides, WT

Accession	Description	Peptide ID dataset I	Peptide ID dataset II	Peptide sequence	Phospho residue(s)	*p*-value dataset I	*p*-value dataset II	*q*-value dataset I	*q*-value dataset II	Peak dataset I	Peak dataset II
AT2G07360	TASH3	2769, 5085	9464, 8286	YQSTYEGYGSPIREE PPPPYSYSEPQSR	10	1.1E-02	2.6E-02	4.9E-02	3.7E-01	24	36
AT4G26130	unknown pr.	5416, 7652, 1518	7456	TTSIGDGGEEGVDDK ASNFINK(FK)	3	1.4E-02	2.6E-02	5.3E-02	3.7E-01	24	40
AT1G44800	nodulin MtN21	7377	34568	SQELPITNVVK	1	4.4E-06	2.6E-02	6.5E-04	3.7E-01	**28**	**52**
AT2G46920	POL	7848	11608	SNFSAPLSFR	8	1.9E-03	3.1E-02	2.3E-02	4.1E-01	28	40
AT2G42600, AT3G14940	PPC2/PPC3	1672, 57	62, 40, 4070	MASIDAQLR	3	7.4E-03	4.0E-02	4.0E-02	4.7E-01	32	24
AT3G60240	EIF4G	1585	1579	QVLQGPSATVNSPR	12	3.8E-03	4.3E-02	3.0E-02	4.9E-01	**28**	**48**
AT1G70770	DUF2359	514	169, 800	MTAIDSDDDGVVR	6	7.4E-03	4.3E-02	4.0E-02	4.9E-01	**24**	**48**
AT5G40890, AT3G27170	CLC-A/CLC-B	749	406	TLSSTPLALVGAK	3	1.3E-04	4.3E-02	6.2E-03	4.9E-01	**28**	**48**
AT4G12770, AT4G12780	AUXILIN-LIKE 1/2.	238, 238	318	FENVFSSISSSPTK	11	6.0E-03	4.7E-02	3.6E-02	5.2E-01	**28**	**48**

B. Phosphopeptides, CCA1-OX

Accession	Description	Peptide ID dataset I	Peptide ID dataset II	Peptide sequence	Phospho residue(s)	*p*-value dataset I	*p*-value dataset II	*q*-value dataset I	*q*-value dataset II	Peak dataset I (h)	Peak dataset II (h)
AT2G33830	DRM2	1348, 43281	2709	TVAAVAGSPGTPTTPGSAR	11	0.023	0.0069	1	1	12	24
AT1G51805	SIF3	2617	2514, 1136	VEGTLPSYMQASDGRSPR	16	0.019	0.021	1	1	**24**	**24**

C. Phosphopeptides, CCA1-OX, allowing periods of 12–20 h

Accession	Description	Peptide ID dataset I	Peptide ID dataset II	Peptide sequence	Phospho residue(s)	*p*-value dataset I	*p*-value dataset II	*q*-value dataset I	*q*-value dataset II	Peak dataset I (h)	Peak dataset II (h)
AT1G77760	NIA1	4776	1968	SVSSPFMNTASK	3	0.013	0.00067	0.42	0.25	**24**	**48**
AT2G45820	REMORIN 1.3	1234, 5319	698, 2343	ALAVVEKPIEEHTPK	13	0.019	0.0045	0.42	0.68	**24**	**24**

D. Global proteomics, WT

Accession	Description	*p*-value dataset I	*p*-value dataset II	*q*-value dataset I	*q*-value dataset II	Peak dataset I (h)	Peak dataset II (h)
AT4G39800	MI-1-P SYNTHASE	6.22E-06	8.7E-12	0.0059	5.78E-09	**28**	**24**
AT4G17090	BAM3	0.0056	4.6E-05	0.23	0.015	**20**	**44**
AT5G13630	GUN5	0.030	0.00010	0.43	0.028	**32**	**52**
AT1G78570	RHM1	0.00045	0.00059	0.071	0.087	**28**	**48**
AT1G15820	LHCB6	0.044	0.023	0.52	0.93	**12**	**36**
AT5G54190 or AT4G27440	PORA or PORB	0.00025	0.030	0.065	1	**12**	**36**
AT3G08940 or AT2G40100	LHCB4.2 or LHCB4.3	0.0013	0.021	0.16	0.88	**12**	**36**
AT2G05070 or AT2G05100	LHCB2.2 or LHCB2.1	0.013	0.00032	0.31	0.062	**12**	**32**

E. Global proteomics, CCA1-OX

Accession	Description	*p*-value dataset I	*p*-value dataset II	*q*-value dataset I	*q*-value dataset II	Peak dataset I (h)	Peak dataset II (h)
AT3G47070	Unknown	0.034	0.012	0.63	0.91	**20**	**40**
AT3G49190	O-acyltransferase fam. pr.	0.0016	0.022	0.24	0.92	32	44
AT4G39800	MI-1-P SYNTHASE	0.00037	0.03406	0.18	0.99	**24**	**24**
AT1G08200 or AT2G27860	AXS2 or AXS1	0.0056	0.0026	0.35	0.56	**20**	**44**

Abbreviations: fam., family; pr, protein.
All *p*-values are based on JTK_CYCLE analysis, and *q*-values are BH-corrected *p*-values.
In some phosphopeptides, the location of phosphorylated residues differs slightly between datasets (shifted by 1–2 residues or one of several phosphates is missing), in which case, the phosphorylated residues of both datasets are noted (dataset I/dataset II).
Bold denotes phase difference of peak is up to 4 h.

Next, we compared our WT datasets with a previously published phosphoproteomics time course in WT seedlings taken from ZT 25 to ZT 45 at 4 h intervals (9) (supplemental Data S7), using FDR corrected ANOVA, since ANOVA was used for statistical analysis in (9). We considered only exactly matched peptide sequences and modifications. Out of 422 modified peptides that were shared between (9) and Phospho I, 20 were rhythmic in both datasets, which is a significant enrichment (Fisher's exact test $p = 0.0031$). Similarly, when comparing (9) with Phospho II, 378 phosphopeptides were detected in both datasets, six were significantly changing in both (Fisher's exact test for over-representation: $p = 0.0019$) (supplemental Data S7). For a more fine-grained analysis, we determined the phase differences of peaks of each phosphopeptide that was identified or detected in both dataset comparisons (supplemental Fig. S2). Especially for the significantly changing phosphopeptides, a majority had a peak phase difference of 1 or 3 h, the adjacent time points given different sampling times in these studies. Overall, this comparison indicates that in spite of differences in developmental stage and methodological approach, the observed dynamics are largely consistent.

Since *CCA1* is a morning-expressed gene, the CCA1-OX line might be expected to have a "morning-locked" circadian oscillator. To test whether this observation applies at the protein abundance and phosphorylation level, we calculated the absolute value of the difference between CCA1-OX and WT (|CCA1-OX - WT|) at each dawn and dusk time point (*i.e.*, ZT12, 24, 36, and 48) for time courses of all proteins or phosphopeptides that were rhythmic in WT (p-value < 0.05) and quantified in CCA1-OX. For each dawn–dusk pair, we determined whether the difference between CCA1-OX and WT was larger at dusk or at dawn and counted the number of such pairs as a coarse indication of the difference between the proteome or phosphoproteome of these two genotypes, for each dataset and time point pair (supplemental Table S2). CCA1-OX differed more from the WT at dusk rather than dawn, in all but one of the time point pairs (the exception was one of the smallest pairs, in global dataset II). This is consistent with a partially morning-locked circadian clock at the protein (modification) level, as expected from the role of CCA1 in the TTFL. The consistency of the dataset supports our interpretation, from the very few rhythmic identifications in CCA1-OX that the TTFL is necessary for most of the rhythms observed in WT plants.

Circadian Rhythms of Proteins in the Global Proteomics Datasets

We applied GO analysis to the global proteomics data, using rhythmic proteins at each peak time point as foreground and all other identified proteins as background (supplemental Data S6). In both datasets, enriched GO terms in the WT at the end of the subjective day (ZT12 and ZT36) were photosynthesis related terms, "response to glucose," "regulation of protein dephosphorylation," and oxidoreductase activity with

NAD or NADP as acceptor. The latter term was also enriched in the CCA1-OX in dataset I. In addition, in the CCA1-OX, two terms related to cell wall metabolic processes were enriched in both datasets during the subjective night (ZT20 and ZT44) (supplemental Data S6).

Among rhythmic proteins shared between datasets I and II, we identified eight within the WT data, and four for the CCA1-OX data (Table 2, *D* and *E*). One protein, INOSITOL 3-PHOSPHATE SYNTHASE 1 (MIPS1, AT4G39800) was rhythmic with a peak at 24–28 h in both datasets and both genotypes but with lower *p*-value and higher amplitude in the WT (Fig. 2*A*). Two other examples of high-confidence rhythms in protein abundance in the WT are chloroplast BETA-AMYLASE 3 (BAM3) (Fig. 2*B*) and the light-harvesting chlorophyll a/b binding protein LHCB2.1/LHCB2.2 (Fig. 2*C*). Two of the proteins that were rhythmic in both CCA1-OX datasets (AT3G47070 and AT3G49190, Table 2*E*) were also rhythmic in one of the WT datasets (JTK_CYCLE *p*-values < 0.05). Though they were not positively identified in WT by our analytical approach, it is therefore unlikely that these proteins are exclusively rhythmic in the CCA1-OX.

WT Phosphoproteomics Data Reveals Rhythmic Phosphoproteins With a Variety of Functions, Including Previously Unknown Phosphosite Rhythms

GO term enrichment within the peak time groups of the phosphoproteomics data revealed that only one GO term ("cotyledon development") was shared between the two datasets and the ZTs of enrichment are 16 h apart (supplemental Data S6). Several terms were shared between the WT and the CCA1-OX in dataset I, most of them related to energy metabolism or ion homeostasis, and all of them were enriched at ZT24 or ZT28. Apart from overlap of exact GO IDs, we found enrichment of terms related to translation in the WT at 24 h in both phosphoproteomics datasets, which is consistent with rhythmic phosphorylation of RPS6 isoforms (supplemental Data S6, Table 2, supplemental Data S3) (9).

In agreement with the small number of consistently enriched GO terms and with (9), we found that the proteins for which we found rhythmic phosphosites in the WT are associated with a large variety of functions, such as translation initiation (RPS6A, RPS6B), nitrogen/amino acid metabolism or transport (NIA2, NRT1.7, CLC-A), light harvesting (CAB4), or flowering (COL-9).

In our datasets we also found previously unknown phosphosite rhythms, such as on ASPARAGINE SYNTHETASE (ASN) 2, SWEET12, PLASMA MEMBRANE INTRINSIC PROTEIN (PIP) 2;7, and VARICOSE RELATED (VCR) (Fig. 3, and see discussion).

Very Few Proteins Are Rhythmically Phosphorylated in the CCA1-OX

Only two phosphopeptides with $p < 0.05$ for the CCA1-OX appear in both datasets (Table 2*B*): A phosphopeptide of a

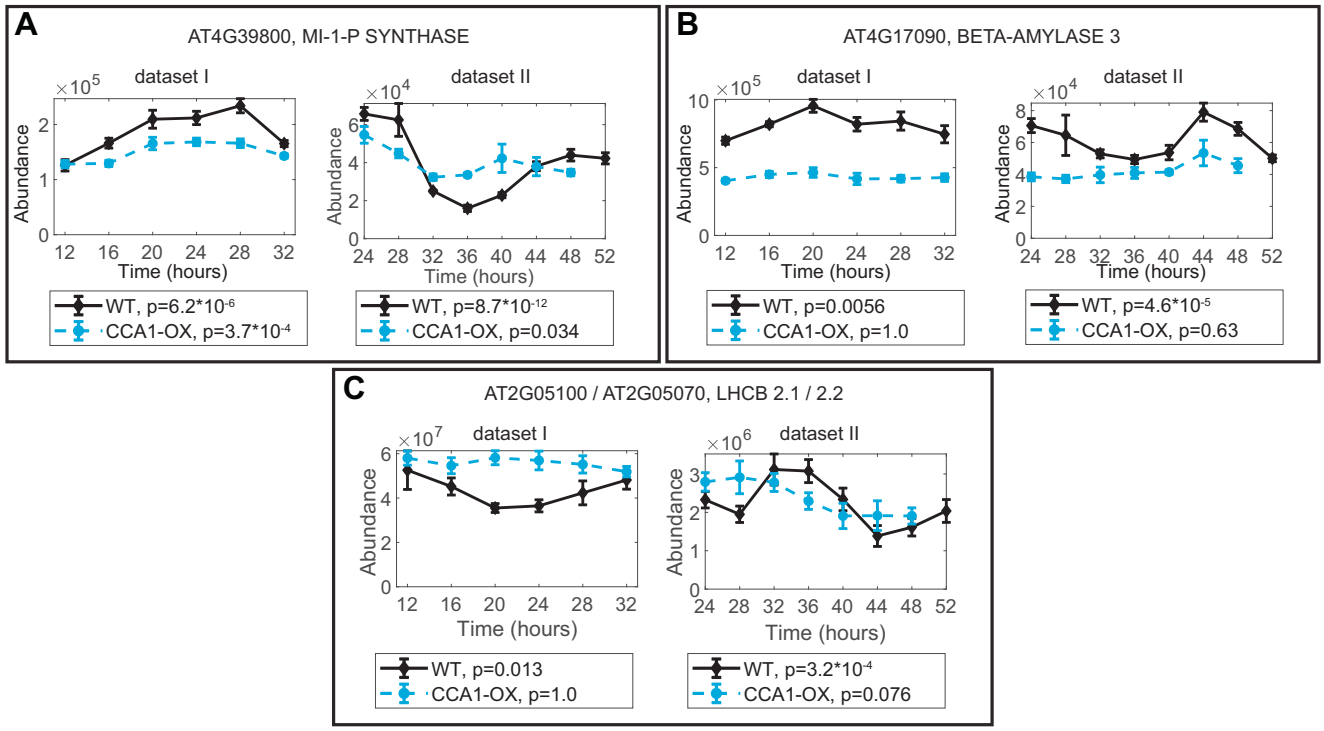

FIG. 2. **Examples of three proteins with rhythmic abundance in both datasets.** *A*, MIPS1, (*B*) BAM3, (*C*) LHCB2.1/2.2. JTK_CYCLE *p*-values are indicated under the graphs.

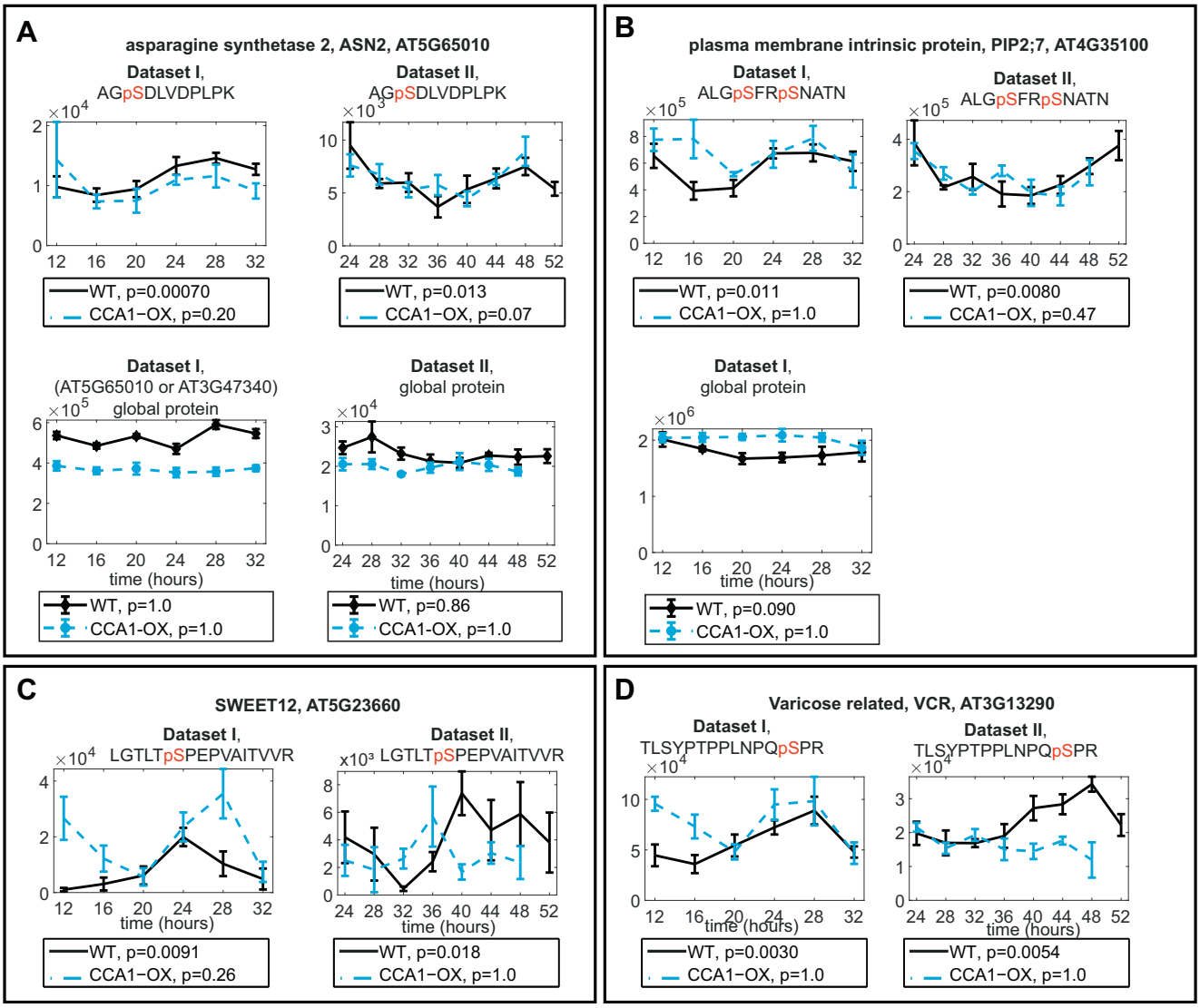

FIG. 3. **Examples of newly described phosphopeptide rhythms with JTK_CYCLE $p < 0.05$ in both datasets.** Phosphopeptide from (*A*) an asparagine synthetase, ASN2, with global protein abundance plots (*B*) from aquaporin PIP2;7 with global protein abundance plot from dataset I (not detected in dataset II) (*C*) from the sucrose efflux protein SWEET12 and (*D*) from VCR. Protein not detected in global proteomics for (*C*) and (*D*). JTK_CYCLE *p*-values are indicated under the graphs.

Leucine-rich repeat protein kinase (AT1G51805) and the dormancy/auxin-associated family protein DRM2 (AT2G33830). The latter showed a significant decrease in its total protein abundance in dataset I (Table 2*B*); therefore changes may be due to decreasing protein expression in constant light.

"Phospho-Dawn": Most Rhythmic Phosphopeptides Peak in the Subjective Morning

Analysis of the number of phosphopeptides that peak at each time point revealed that 45% (dataset I) and 73% (dataset II) of rhythmic phosphopeptides peak around subjective dawn in the WT (Figs. 4*A* and 5, *A* and *B*). This is in agreement with previous observations in *Ostreococcus* and *Arabidopsis* (9, 43). By contrast, in the global proteomics dataset, no tendency for increased abundance at dawn was observed (Figs. 4*C* and 5, *C* and *D*). These observations hold true when using an alternative ANOVA analysis, detecting change rather than rhythmicity, with a *p*-value cutoff of $p < 0.05$ (supplemental Fig. S3). Therefore, the preponderance of "phospho dawn" patterns is more likely due to (de)phosphorylation events rather than to changes in the abundance of the cognate proteins.

Interestingly, almost all of the few phosphopeptides with JTK_CYCLE *p*-value < 0.05 also peaked at subjective dawn in the CCA1-OX plants (Figs. 4*B* and 5, *A* and *B*, supplemental Fig. S3), which suggests residual rhythmicity phased similarly to the WT. To expand the search for rhythms in the CCA1-OX, we tested whether there are rhythmic phosphopeptides with

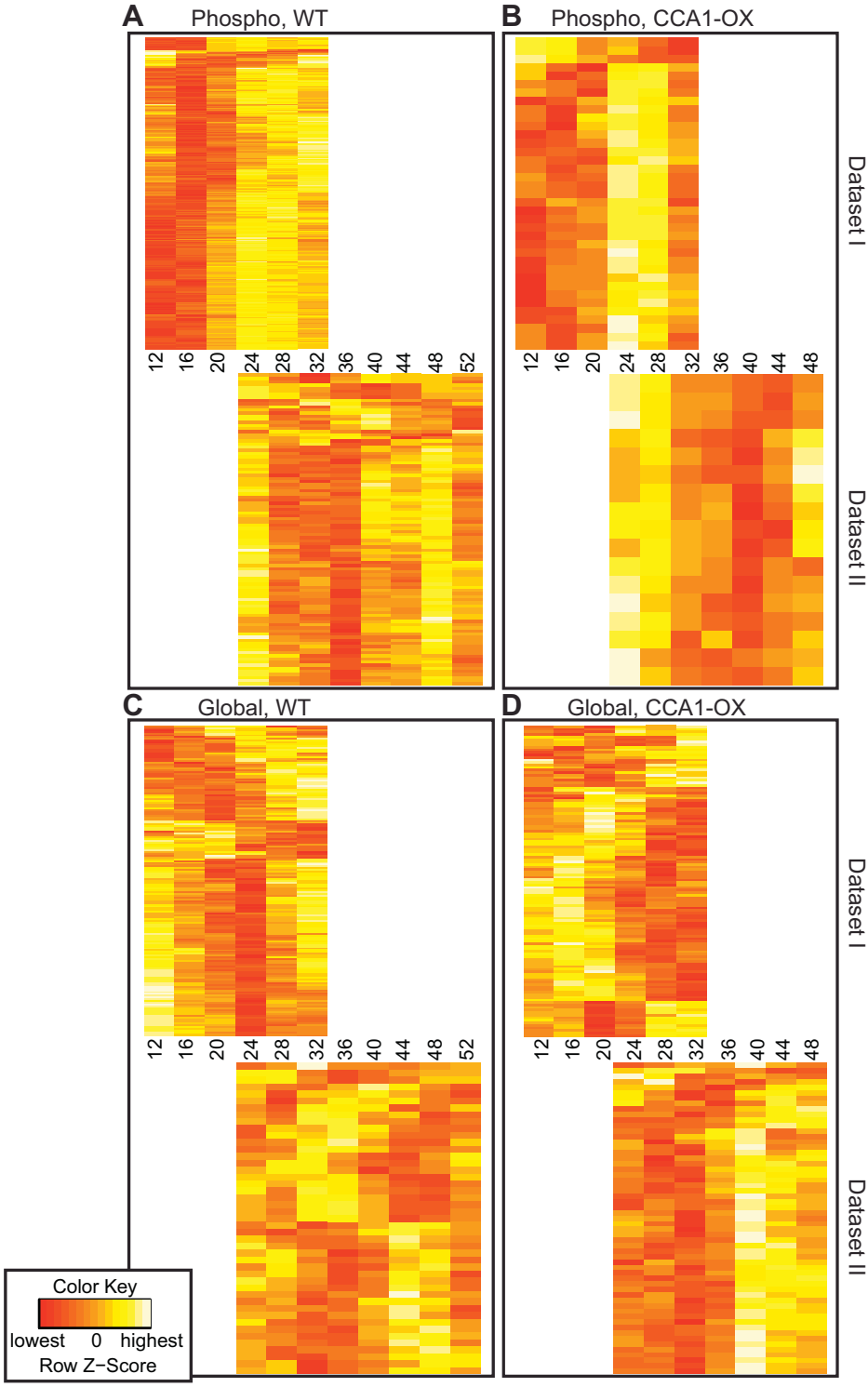

FIG. 4. **Whole-dataset protein and phosphopeptide dynamics.** Heatmaps were generated by hierarchical clustering of phosphopeptide (*A* and *B*) or global protein (*C* and *D*) abundance time courses in dataset I and II (indicated on the *right*) for WT (*A* and *C*) and CCA1-OX (*B* and *D*).

shorter periods that would have been excluded from the analysis above. We repeated the JTK_CYCLE analysis, allowing periods down to 12 h. Hardly any phosphopeptides had periods of less than 22 h in the WT, while the majority of phosphopeptides had a predicted period of 12 or 16 h in the CCA1-OX (Fig. 5, *E* and *F*). Interestingly, the majority of those short-period rhythmic phosphopeptides also peaked at 24 h or 48 h (Fig. 5, *A* and *B*). In conclusion, in both of our independent

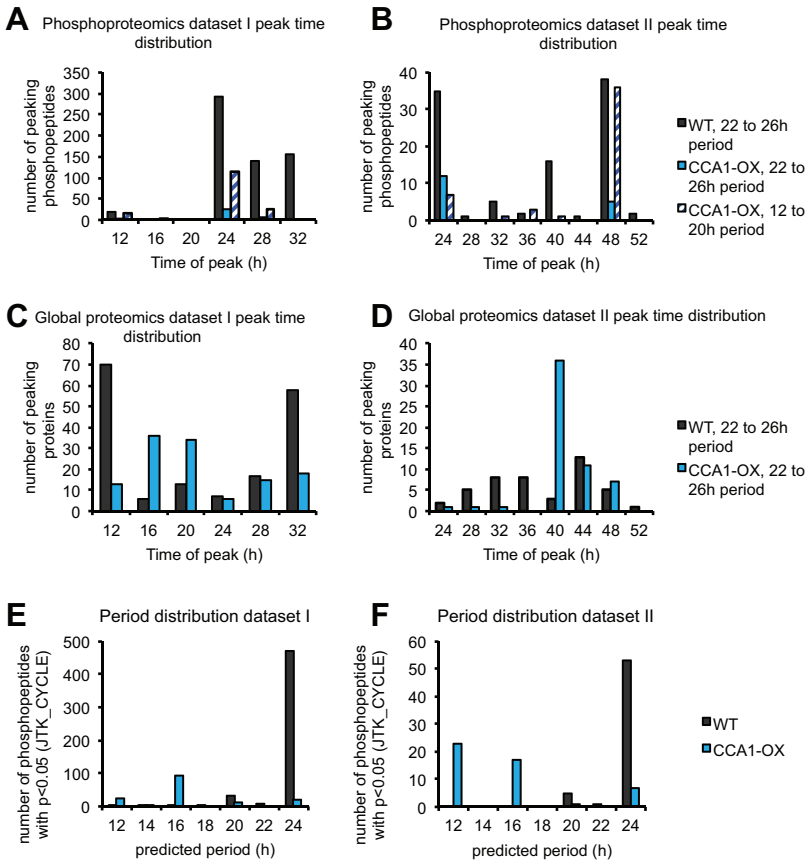

FIG. 5. **Peak time and period distribution of phosphopeptide and global protein time courses.** *A–D*, number of rhythmic (JTK_CYCLE *p*-value < 0.05) phosphopeptides (*A* and *B*) or proteins (*C* and *D*) peaking at each time point, allowing a period of around 24 h (22–26) or 12 to 20 h. *E* and *F*, periods according to JTK_CYCLE allowing periods from 12 to 24 h for phosphoproteomics dataset I (*E*) and II (*F*). Number of rhythmic phosphopeptides (JTK_CYCLE *p*-value < 0.05) for each predicted period is plotted.

WT phosphoproteomics datasets, the majority of phosphopeptides peak around subjective dawn, and this "phospho dawn" may not be completely abolished by disruption of the TTFL.

Kinase Prediction Suggests CDPK/SnRK Family Members Target Dawn Phased Phosphopeptides

We reasoned that there may be a kinase activity that is present predominantly around subjective dawn, which is either very robustly dawn-timed by the TTFL even when it is strongly impaired, or an alternative oscillator, such as an NTO, contributes to the dawn phased kinase activity. Characterization of the phospho-dawn peptides could help to identify either a very robust dawn-phased TTFL output, or potentially consequences of an NTO. For this reason, we focused on the dawn peaking phosphopeptides to identify candidate kinases, using phosphosite motif analysis and kinase prediction. In these analyses we used the ZT24 or ZT48 peaking rhythmic (JTK_CYCLE *p*-value < 0.05) phosphopeptides as foreground and all other identified phosphopeptides as background. No target site motifs were significantly overrepresented in a consistent way between datasets (supplemental Figs. S4 and S5). For predicting candidate kinases, we searched for enrichment of kinase groups that target phosphopeptides with JTK_CYCLE *p*-value < 0.05 (Table 3) using the GPS3 resource. In the WT, both datasets share enrichment of CMGC kinase groups such as MAPK and CAMK groups. The latter caught our attention since it is the only consistently enriched group in both genotypes and both datasets. The CAMK group was also consistently enriched among significantly changing phosphopeptides scored using ANOVA *p*-value < 0.05 (supplemental Table S3).

The CAMK group in plants contains the CDPK/SnRK family of kinases with 89 members (44) in the EKPD database (45) that informs GPS3. Interestingly, among the phospho dawn peptides we found phosphosites that may be direct or indirect SnRK1 target proteins according to two proteomics studies (46, 47): NITRATE REDUCTASE (NIA) 1 and 2 and the bifunctional enzyme F2KP (supplemental Fig. S6 and supplemental Table S4). Interestingly, nitrate reductases have

TABLE 3
Summary of GPS3 kinase prediction followed by Fisher's exact test

A. Dataset I

Time point	WT, 22- to 26-h period				CCA1-OX, 22- to 26-h period			CCA1-OX, 12- to 20-h period
	Peak		Trough	All $p < 0.05$	Peak	Trough	All $p < 0.05$	Peak
	24 h	28 h	12 h		24 h	12 h		24 h
AGC					0.043			
AGC/NDR		0.0072						
Atypical/TAF1	6.50E-06		2.50E-06					
CAMK		0.0012		0.0040		0.00063	0.0090	0.024
CAMK/DAPK								0.029
CMGC/CK2	0.0012		4.70E-06					
CMGC/MAPK				0.027				
Other/ULK			0.040			0.0030	0.0066	
Other/WNK								0.044

B. Dataset II

Time point	WT, 22- to 26-h period			CCA1-OX, 22- to 26-h period		CCA1-OX, 12- to 20-h period
	Peak		All $p < 0.05$	Peak	All $p < 0.05$	Peak
	24 h	48 h		24 h		24 h
AGC	1.4E-06					
AGC/PDK1	0.0049					
CAMK	0.00024		0.0049			0.048
CAMK-L						0.0035
CAMK-Unique	0.057					
CMGC	0.0061			0.040		
CMGC/GSK	0.0078					
CMGC/MAPK		0.040				
Other/PEK				0.028	0.047	
STE/STE7	0.037					

Fisher's exact test *p*-values for enrichment of each kinase group are shown. Foreground groups were chosen with JTK_CYCLE *p*-values < 0.05 and peaks or troughs at indicated ZTs.

been reported as classical SnRK1 targets in other species (48). In light–dark cycles, NIA1 and NIA2 protein abundances are rhythmic (25), while in our analysis under constant light NIA1 protein was not detected in the global analysis and NIA2 protein abundance changed significantly (supplemental Fig. S4*B*) but not in phase with the phosphosites, suggestive of regulated (de)phosphorylation. Another indication of increased SnRK1 activity at subjective dawn are rhythms in phosphopeptides and abundance of the protein FCS-LIKE ZINC FINGER (FLZ)6 (supplemental Fig. S7): transcriptional upregulation of *FLZ6* by SnRK1 signaling has previously been shown (49, 50). In a dataset with WT seedlings in constant light (51), the *FLZ6* transcript peaks 4 h before the FLZ6 protein in our dataset.

Rhythmically Phosphorylated Kinases and Phosphatases

Since kinases and phosphatases themselves can be regulated by phosphorylation, we were interested in rhythmic phosphopeptides of kinases and phosphatases. Identification of rhythmic kinase or phosphatase activities in the WT could help to discover components of clock output pathways that are mediated *via* protein phosphorylation.

For two kinases, CRK8 and AT5G61560, we found rhythmic phosphopeptides in the WT where protein abundance did not oscillate in parallel, indicating that rhythmicity is due to phosphorylation rather than changes in protein abundance (supplemental Fig. S8). CRK8 is a member of the CDPK-SnRK1 superfamily (44). To our knowledge, no specific functions have been investigated for either of these kinases.

All rhythmically phosphorylated phosphatases in our data are members of the protein phosphatase 2C (PP2C) family (supplemental Fig. S9) and were classified as rhythmic only in the WT. PP2C G1 (supplemental Fig. S9*A*) is involved in ABA dependent salt stress response and, in contrast to PP2CAs, is a positive ABA signaling regulator (52) but to our knowledge, no reports exist on the functional relevance of its own phosphorylation. AT3G51470 is also a PP2CG family member, was only rhythmic in dataset I, and no functional information is available (53). The final PP2C POLTERGEIST (POL, supplemental Fig. S9*C*) is involved in stem cell regulation (54).

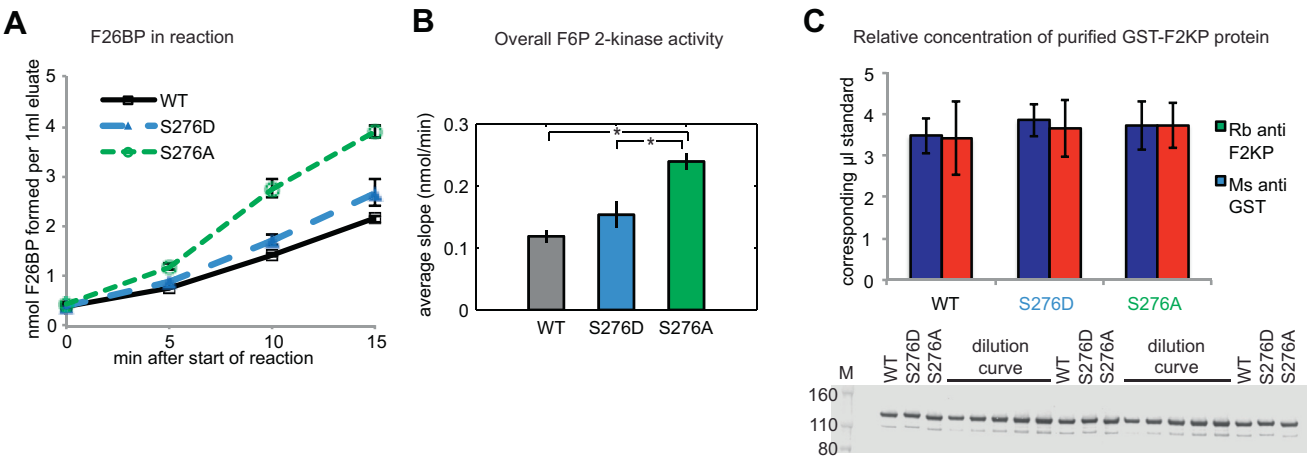

FIG. 6. ***In vitro* GST-F2KP activity assay with WT and Ser276 point mutations.** *A*, fructose-2,6-bisphosphate (F26BP)) accumulation during the reaction. *B*, kinase activity calculated from slopes in (*A*). *C*, relative quantification of GST-F2KP in eluates probed with rabbit (Rb) anti F2KP and mouse (Ms) anti GST. Protein blot is shown below quantification for rabbit anti F2KP. A dilution series of a sample mix was used for quantification, ranging from 0.5 to 1.5 loading equivalent of the samples. Averages of both dilution curves were used. Error bars: SEM. **p*-value < 0.05 in *t* test.

In the CCA1-OX data, the profiles for the kinases and phosphatases discussed above can show some similarity to the WT pattern, but none were classified as rhythmic by JTK_CYCLE. The biochemical mechanisms underlying the relatively robust phosphoprotein rhythms in the WT should prove easier to investigate than any remaining rhythmicity in the CCA1-OX.

Phospho-Null Mutation of Ser276 of the Enzyme F2KP Enhances F6P-2kinase Activity In vitro

As an example of how our datasets can be used to investigate new clock output pathways, we analyzed the molecular function of a phosphosite of the bifunctional enzyme F2KP. Several phosphosites were detected in F2KP with only Ser276 showing a circadian rhythm in the WT, in dataset II only but at a very high significance level (supplemental Fig. S6*C*, supplemental Data S3). One F2KP peptide was detected in the global protein analysis of dataset II. Its changes over the timecourse are not significant and do not parallel the Ser276 phosphopeptide; therefore it is unlikely that the rhythm in Ser276 phosphorylation is caused by changes in F2KP protein abundance.

We tested whether the Ser276 phosphorylation site is relevant for F2KP function, since this site is highly conserved with other plant species (supplemental Fig. S10*A*), and a very specific enzymatic assay has been described (41, 55). Maximum F6P,2K activity was measured of GST-tagged phosphomimetic mutants S276D and S276A, and the unmutated WT control enzyme *in vitro*. Two independent preparations (bacterial expression and purification using a GST tag) were tested to ensure reproducibility. Equivalence of the amounts of expressed F2KP protein in assays was verified by western blotting with two different antibodies (Fig. 6*C*, supplemental Fig. S10*D*). S276A had an approximately 2.5-fold increased activity compared with the unmutated version, while S276D had only slightly increased activity (Fig. 6, *A* and *B*, supplemental Fig. S10, *B*, *C*, and *E*). The rhythmicity observed at this phosphosite is therefore consistent with a rhythmic input to F2KP function in central carbon metabolism.

DISCUSSION

This study focuses on global and phospho-proteomic timeseries in *Arabidopsis* plants harvested under constant light conditions, where rhythmicity is driven by the circadian clock. In WT plants, we tested the prevalence of circadian rhythms in protein phosphorylation and abundance, which has rarely been reported. In the CCA1-OX transgenic line, we tested the importance of the clock gene circuit for that rhythmic regulation, given that markers of a Non-Transcriptional Oscillator (NTO) are rhythmic in Arabidopsis, and that protein phosphorylation drives the best-characterized NTO in cyanobacteria.

Could an NTO Contribute to the Phospho-Dawn?

CCA1-OX transgenic lines have been widely used as an approximation of a plant without a functional clock. In this line we found very few rhythmic phosphopeptides and proteins, and those with statistical significance typically had less convincing waveforms than rhythms in the WT (Table 1). Therefore, if an NTO exists in *Arabidopsis*, it confers rhythmicity only to very few of the phosphosites we detected. Intriguingly, in both datasets, we still observe the phospho-dawn phenomenon in the CCA1-OX (Figs. 4 and 5, supplemental Fig. S3), whereas a uniform phase distribution would be expected in the noise-driven fluctuations of an

arrhythmic plant. It remains possible that an NTO controls this fraction of dawn-phased phosphorylation, albeit too weakly to yield robust rhythms, whereas the majority of phosphoprotein rhythmicity requires a functioning clock gene circuit. We cannot exclude that some rhythmicity of that canonical gene circuit remains even in the CCA1-OX, for example, as the CaMV 35S promoter does not confer strong expression in all tissues (55). Additional experiments, such as phosphoproteomics in other arrhythmic mutants, testing other post-translational markers such as redox modifications, and identifying NTO outputs other than PRX overoxidation (19) and Mg^{2+} rhythms (20, 21) might further define the effects of a potential NTO in *Arabidopsis*.

Proteins With Rhythmic Abundance

We found that the proportion of rhythmic phosphopeptides is larger than for protein abundance, but smaller than for rhythmic transcripts (Table 1). The set of rhythmic proteins does not support extensive inference, though we note that the three examples of rhythmic proteins in Figure 2 all follow the rhythmic regulation of their cognate transcripts. MIPS1 (Fig. 2*A*) is transcriptionally induced by light, acting through FAR-RED ELONGATED HYPOCOTYLS (FHY)3 and FAR-RED IMPAIRED RESPONSE (FAR)1 at the transition from darkness to light in light–dark cycles and enhances myo-inositol abundance, which in turn limits oxidative stress at the onset of photosynthesis (56, 57). Rhythmic *MIPS1* transcript abundance peaks toward the end of the subjective night in constant light (58, 59), before a protein peak shortly after subjective dawn. The rhythmic control of MIPS1 abundance is consistent with anticipation of light-induced oxidative stress, providing a potential physiological function in addition to the subsequent, light-responsive induction of myo-inositol production.

BAM3 (Fig. 2*B*) is the dominant beta-amylase contributing to starch degradation (60). The circadian clock is key for the timing of night-time starch degradation (61). In light–dark cycles, *BAM3* transcript abundance drops at the beginning of the day and increases during the night (62, 63), and this pattern persists in constant light (58, 59). We observe a protein abundance pattern that matches the transcript dynamics, indicating that the transcriptional control may be responsible for the protein rhythm. This is also the case for LHCB2.1/2.2 (Fig. 2*C*), a component of the photosystem II light harvesting complex (59).

Proteins With Newly Discovered Phosphopeptide Rhythms

We show four examples of newly discovered phosphopeptide rhythms in Figure 3. ASN2 (Fig. 3*A*) is one out of three described *Arabidopsis* asparagine synthetases, which catalyze the transfer of an amino group from glutamine to aspartate, producing asparagine and glutamate, but ASN2 may also directly use ammonia as a substrate (64, 65). The two most expressed asparagine synthetase enzymes in Arabidopsis are ASN1 and ASN2 (64), and in contrast to ASN1, the physiological function of ASN2 is less well understood. We did not find any evidence for ASN2 protein abundance rhythms (Fig. 3*A*), indicating that the phosphosite's peak near subjective dawn is due to rhythmic kinase and/or phosphatase action. Interestingly, the ammonia transporter AMT1;1 also has a rhythmic phosphosite with a temporal profile that parallels the ASN2 peptide (supplemental Data S3, Table 2). The presence of rhythmic phosphosites of proteins involved in nitrate metabolism or transport in our data and (9) supports the notion that nitrogen-related processes are under control of the circadian clock at the posttranslational level, in part through rhythmic AMT1;1 and ASN2 phosphorylation.

In water transport, our results demonstrate a previously undiscovered phosphosite rhythm on the aquaporin PLASMA MEMBRANE INTRINSIC PROTEIN (PIP)2;7 (Fig. 3*B*). According to (66), this phosphosite is a CPK1 and CPK34 target, and its abundance decreases in response to ABA treatment (67). In response to salt stress, the entire protein is internalized from the plasma membrane, with a concomitant reduction in hydraulic conductivity (68), indicating that decreasing PIP2;7 activity limits water loss. Rhythmic phosphorylation of other aquaporins was previously demonstrated in constant light or darkness (9, 69). Therefore, PIP2;7 may, together with other aquaporins, mediate circadian clock regulation of hydraulic conductivity or high salinity response through its phosphorylation status.

In carbon transport, a newly discovered phosphosite rhythm was found for the sucrose efflux transporter SWEET12 (Fig. 3*C*) (70). To our knowledge, the function of this phosphosite is unknown, but one may speculate that this rhythm could reflect circadian control of carbon reallocation.

Finally, we have high confidence in the rhythmicity of a phosphopeptide of the putative RNA decapping protein VARICOSE RELATED (VCR) (Fig. 3*D*). VCR and its close homologue VARICOSE (VCS) interact with and are phosphorylated by SnRK2.6 and SnRK2.10 at several serines (71, 72). While the VCR phosphosite shown in Figure 3*D* is not one of the phosphosites identified by (72), SnRK2.10 phosphorylates an almost identical site on VCS (TLSYPTPPLNLQpSPR). Therefore, it is very likely that the corresponding site on VCR is also a SnRK2.10 target.

Altogether, these examples demonstrate how our data can be used to generate hypotheses on clock output pathways affecting different aspects of plant physiology through phosphorylation.

A Rhythmic F2KP Phosphosite Is Biochemically Relevant

The specific roles of most of the rhythmic phosphorylation sites identified in our study have not been investigated. To exemplify in an experimental approach how circadian phosphorylation of a protein can be linked to its function, we analyzed the effect of a phosphosite mutation on the activity of the enzyme F2KP. F2KP is one of the regulators of carbon partitioning into starch and sucrose (73) and is necessary to

maintain normal growth in fluctuating light conditions (74). With its kinase domain it can synthesize F-2,6-BP from F-6-P, and with its phosphatase domain it catalyzes the reverse reaction (73).

The phosphosite of interest, Ser276, is within the plant-specific regulatory N-terminal domain (42, 75) but is not among the phosphosites in the known 14-3-3 binding site (76). Ser276 is regulated by SnRK1 (46) and is conserved in many plant species (supplemental Fig. S10*A*).

Our *in-vitro* F-6-P,2 kinase activity measurement experiments showed that substitution of Ser276 by Ala increases F2KP's kinase activity. It is unknown whether *in vitro* expressed F2KP is phosphorylated at Ser276 or not. However, comparison of Ser276 mutation to Ala with the WT and with mutation to Asp, suggests that a lack of negative charge at position 276 leads to increased kinase activity. In dataset II, pSer276 decreased gradually during the subjective day (supplemental Fig. S6*C*). Assuming that the phospho mimic/WT and null mutations reflect the behavior of the phosphorylated and nonphosphorylated site, respectively, we extrapolate that toward the end of the day, more F-2,6-BP is produced, and therefore starch synthesis is favored over UDP-glucose and sucrose synthesis. Indeed, F-2,6-BP levels in the plant increase slowly across the day in short day conditions (76). Testing the function of these mutations *in planta* will be interesting to determine whether this phosphosite has physiological relevance, in addition to biochemical effectiveness.

Phospho-Dawn Is Likely Mediated by Several Different Kinases

We aimed to characterize the phospho-dawn phenomenon as it may point to novel dawn-specific circadian clock output through posttranslational mechanisms. Although the striking abundance of dawn-phased phosphopeptides could partly be biased toward the easily detectable or abundant phosphopeptides of our dataset, it is consistent with highest transcript expression of kinases and phosphatases at the end of the night in diel time courses (26, 77).

Our kinase prediction revealed enrichment of some CMGC subgroups, such as MAPK, CK2, GSK, DYRK, CDK, or DAPK. CK2 is involved in the circadian clock function in Arabidopsis by phosphorylating CCA1 (4, 78). A previous study reported enrichment of predominantly CK2 predictions among significantly changing phosphopeptides (9). Roles for MAPK and GSK have been reported for the circadian clock function in other eukaryotes (79–82). However, the most consistently enriched group of kinases at subjective dawn in our datasets is the CAMK group (Table 3, supplemental Table S3), which comprises the 89 members of the CDPK-SnRK superfamily of kinases.

All of these 89 CDPK-SnRK members are potential candidates for causing the observed phospho-dawn. Not all of these kinases have been studied in much detail, and for the majority of rhythmic phosphopeptides no experimental evidence for kinase specificities exists. However, making use of literature on existing kinase–target pairs can help to narrow down candidates. For example, as mentioned above, CPK1, CPK34, and likely SnRK2.10 phosphorylate dawn-peaking phosphosites shown in Figure 3. In addition, SnRK and CPK/CDPK kinases can themselves be regulated by phosphorylation (44). CRK8, of which we found a very prominently dawn-peaking rhythmic phosphopeptide (supplemental Fig. S8*A*), is therefore another candidate phospho-dawn kinase.

We also show that several previously reported SnRK1 regulated sites are rhythmic with peaks around subjective dawn including phosphopeptides of F2KP and nitrate reductases NIA1 and NIA2 (supplemental Fig. S6). Additional indication comes from the protein FLZ6, which is transcriptionally induced by and interacts with SnRK1 and may serve as a platform for SnRK1 signaling (83). FLZ6 protein abundance and two phosphopeptides were rhythmic in the WT with a peak around subjective dawn (supplemental Fig. S7). SnRK1 may be a particularly relevant candidate as its involvement in circadian timing has previously been reported (84–86) and as it is an important metabolic hub. In normal light–dark conditions, the morning is associated with profound metabolic changes in plants, such as the transition from using starch to direct photoassimilates, or to the alternative, a starvation response if light intensities remain low while starch is almost depleted.

SnRK1 signaling is regarded as antagonistic to TOR signaling (47). Nevertheless, RPS6A and RPS6B phosphosites that are targets of the TOR signaling kinase S6K are rhythmically phosphorylated in the WT and in dataset I also in the CCA1-OX (Table 2, supplemental Data S3 and (9)), with peaks at subjective dawn. This adds to growing evidence that the interplay between SnRK1 and TOR may be more complex than simply antagonistic (87). In fact, the abovementioned SnRK1 induced FLZ6 negatively feeds back to SnRK1, and this has been suggested as a mechanism to allow sufficient TOR activity in spite of high SnRK1 activity (50), which may allow RPS6 phosphorylation to peak at approximately the same time as SnRK1 activity.

Altogether, the identities of the phospho dawn peptides in our study, along with their known and predicted kinases, suggest that phospho-dawn is caused not by a single kinase but several members of the SnRK-CDPK family and also potentially kinases outside this family such as S6K. Further experimentation is required to give evidence for involvement of any such kinases in phospho-dawn, such as time courses of kinase activity and time-resolved phosphoproteomics in mutants of specific candidate kinases. Finding mechanisms that connect the canonical oscillator to prominent post-translational changes at dawn could reveal major clock output pathways that may control a wide range of physiological functions and expand our understanding of how the circadian oscillator increases plant fitness.

DATA AVAILABILITY

The data are publicly available in the pep2pro database (33) at http://fgcz-pep2pro.uzh.ch (Assembly names "ed.ac.uk Global I," "ed.ac.uk Global II," "ed.ac.uk Phospho I," "ed.ac.uk Phospho II") and have been deposited to the ProteomeXchange Consortium (http://proteomecentral.proteomexchange.org) *via* the PRIDE partner repository (34) with the dataset identifier PXD009230. Exported.csv files from Progenesis with all peptide and protein quantifications can be found in the supplemental data (supplemental Data S1 and S2).

Supplemental data—This article contains supplemental data (46, 47, 88–90).

Acknowledgments—We thank Lisa Imrie and Katalin Kis for expert technical support. This research was funded in whole, or in part, by the Wellcome Trust [096995/Z/11/Z]. For the purpose of open access, the authors have applied a CC BY public copyright licence to any author-accepted manuscript version arising from this submission. In addition, this work was supported by BBSRC awards (BB/D019621 and BB/J009423).

Author contributions—J. K., T. H. N., T. L. B., and A. J. M. conceptualization; J. K., T. L. B., and A. J. M. data curation; J. K., M. H., T. H. N., and T. L. B., formal analysis; J. K., K. J. H. and A. J. M, funding acquisition; J. K., L. K. P., and T. L. B., investigation; J. K., L. K. P., H. K. M., T. H. N., T. L. B., and A. J. M. methodology; A. J. M. project administration; T. H. N., K. J. H., T. L. B., and A. J. M. resources; J. K. and M. H. software; T. H. N., K. J. H., G. v. O., T. L. B., and A. J. M. supervision; J. K. visualization; J. K. and A. J. M., writing–original draft; J. K., L. P., T. H. N., G. v. O., T. L. B., and A. J. M. writing–review and editing.

Conflict of interest—The authors declare no competing interests.

Abbreviations—The abbreviations used are: BH, Benjamini–Hochberg; CCA1, Circadian clock associated 1; CCA1-OX, CCA1 overexpressor; CK, casein kinase; Col-0, Columbia 0; F2KP, fructose-6-phosphate-2-kinase/phosphatase; GO, gene ontology; NTO, nontranscriptional oscillator; PCA, principal component analysis; PRX, peroxiredoxin; SEM, standard error of the mean; SNF-1, sucrose nonfermenting; SnRK, SNF-1 related kinase; TTFL, transcriptional translational feedback loop; WT, wild-type; ZT, Zeitgeber time.

Received April 15, 2021, and in revised from, September 27, 2021
Published, MCPRO Papers in Press, November 3, 2021, https://doi.org/10.1016/j.mcpro.2021.100172

REFERENCES

1. Pokhilko, A., Fernández, A. P., Edwards, K. D., Southern, M. M., Halliday, K. J., and Millar, A. J. (2012) The clock gene circuit in Arabidopsis includes a repressilator with additional feedback loops. *Mol. Syst. Biol.* **8**, 574
2. Fogelmark, K., and Troein, C. (2014) Rethinking transcriptional activation in the arabidopsis circadian clock. *PLoS Comput. Biol.* **10**, e1003705
3. van Ooijen, G., and Millar, A. J. (2012) Non-transcriptional oscillators in circadian timekeeping. *Trends Biochem. Sci.* **37**, 484–492
4. Daniel, X., Sugano, S., and Tobin, E. M. (2004) CK2 phosphorylation of CCA1 is necessary for its circadian oscillator function in Arabidopsis. *Proc. Natl. Acad. Sci. U. S. A.* **101**, 3292–3297
5. Nishiwaki, T., Satomi, Y., Nakajima, M., Lee, C., Kiyohara, R., Kageyama, H., Kitayama, Y., Temamoto, M., Yamaguchi, A., Hijikata, A., Go, M., Iwasaki, H., Takao, T., and Kondo, T. (2004) Role of KaiC phosphorylation in the circadian clock system of Synechococcus elongatus PCC 7942. *Proc. Natl. Acad. Sci. U. S. A.* **101**, 13927–13932
6. Maier, B., Wendt, S., Vanselow, J. T., Wallach, T., Reischl, S., Oehmke, S., Schlosser, A., and Kramer, A. (2009) A large-scale functional RNAi screen reveals a role for CK2 in the mammalian circadian clock. *Genes Dev.* **23**, 708–718
7. Yang, Y., Cheng, P., He, Q., Wang, L., and Liu, Y. (2003) Phosphorylation of frequency protein by casein kinase II is necessary for the function of the Neurospora circadian clock. *Mol. Cell. Biol.* **23**, 6221–6228
8. Kusakina, J., and Dodd, A. N. (2012) Phosphorylation in the plant circadian system. *Trends Plant Sci.* **17**, 575–583
9. Choudhary, M. K., Nomura, Y., Wang, L., Nakagami, H., and Somers, D. E. (2015) Quantitative circadian phosphoproteomic analysis of Arabidopsis reveals extensive clock control of key components in physiological, metabolic and signaling pathways. *Mol. Cell. Proteomics* **14**, 2243–2260
10. Leloup, J. C., and Goldbeter, A. (2003) Toward a detailed computational model for the mammalian circadian clock. *Proc. Natl. Acad. Sci. U. S. A.* **100**, 7051–7056
11. Baker, C. L., Loros, J. J., and Dunlap, J. C. (2012) The circadian clock of Neurospora crassa. *FEMS Microbiol. Rev.* **36**, 95–110
12. Takahashi, J. S. (2017) Transcriptional architecture of the mammalian circadian clock. *Nat. Rev. Genet.* **18**, 164–179
13. Mauvoisin, D., Wang, J., Jouffe, C., Martin, E., Atger, F., Waridel, P., Quadroni, M., Gachon, F., and Naef, F. (2014) Circadian clock-dependent and -independent rhythmic proteomes implement distinct diurnal functions in mouse liver. *Proc. Natl. Acad. Sci. U. S. A.* **111**, 167–172
14. Lück, S., Thurley, K., Thaben, P. F., and Westermark, P. O. (2014) Rhythmic degradation explains and unifies circadian transcriptome and proteome data. *Cell Rep.* **9**, 741–751
15. Choudhary, M. K., Nomura, Y., Shi, H., Nakagami, H., and Somers, D. E. (2016) Circadian profiling of the arabidopsis proteome using 2D-DIGE. *Front. Plant Sci.* **7**, 1007–1014
16. Nakajima, M., Imai, K., Ito, H., Nishiwaki, T., Murayama, Y., Iwasaki, H., Oyama, T., and Kondo, T. (2005) Reconstitution of circadian oscillation of cyanobacterial KaiC phosphorylation in vitro. *Science* **308**, 414–415
17. O'Neill, J. S., van Ooijen, G., Dixon, L. E., Troein, C., Corellou, F., Bouget, F. Y., Reddy, A. B., and Millar, A. J. (2011) Circadian rhythms persist without transcription in a eukaryote. *Nature* **469**, 554–558
18. O'Neill, J. S., and Reddy, A. B. (2011) Circadian clocks in human red blood cells. *Nature* **469**, 498–503
19. Edgar, R. S., Green, E. W., Zhao, Y., van Ooijen, G., Olmedo, M., Qin, X., Xu, Y., Pan, M., Valekunja, U. K., Feeney, K. A., Maywood, E. S., Hastings, M. H., Baliga, N. S., Merrow, M., Millar, A. J., *et al.* (2012) Peroxiredoxins are conserved markers of circadian rhythms. *Nature* **485**, 459–464
20. Feeney, K. A., Hansen, L. L., Putker, M., Olivares-Yañez, C., Day, J., Eades, L. J., Larrondo, L. F., Hoyle, N. P., O'Neill, J. S., and van Ooijen, G. (2016) Daily magnesium fluxes regulate cellular timekeeping and energy balance. *Nature* **532**, 375–379
21. Henslee, E. A., Crosby, P., Kitcatt, S. J., Parry, J. S. W., Bernardini, A., Abdallat, R. G., Braun, G., Fatoyinbo, H. O., Harrison, E. J., Edgar, R. S., Hoettges, K. F., Reddy, A. B., Jabr, R. I., von Schantz, M., O'Neill, J. S., *et al.* (2017) Rhythmic potassium transport regulates the circadian clock in human red blood cells. *Nat. Commun.* **8**, 1978
22. Reddy, A. B., Karp, N. A., Maywood, E. S., Sage, E. A., Deery, M., O'Neill, J. S., Wong, G. K., Chesham, J., Odell, M., Lilley, K. S., Kyriacou, C. P., and Hastings, M. H. (2006) Circadian orchestration of the hepatic proteome. *Curr. Biol.* **16**, 1107–1115

23. Robles, M. S., Cox, J., and Mann, M. (2014) In-vivo quantitative proteomics reveals a key contribution of post-transcriptional mechanisms to the circadian regulation of liver metabolism. *PLoS Genet.* **10**, e1004047
24. Robles, M. S., Humphrey, S. J., and Mann, M. (2017) Phosphorylation is a central mechanism for circadian control of metabolism and physiology. *Cell Metab.* **25**, 118–127
25. Uhrig, R. G., Echevarría-Zomeño, S., Schlapfer, P., Grossmann, J., Roschitzki, B., Koerber, N., Fiorani, F., and Gruissem, W. (2021) Diurnal dynamics of the Arabidopsis rosette proteome and phosphoproteome. *Plant Cell Environ.* **44**, 821–841
26. Uhrig, R. G., Schläpfer, P., Roschitzki, B., Hirsch-Hoffmann, M., and Gruissem, W. (2019) Diurnal changes in concerted plant protein phosphorylation and acetylation in Arabidopsis organs and seedlings. *Plant J.* **99**, 176–194
27. Wang, Z. Y., and Tobin, E. M. (1998) Constitutive expression of the circadian clock associated 1 (CCA1) gene disrupts circadian rhythms and suppresses its own expression. *Cell* **93**, 1207–1217
28. Yakir, E., Hassidim, M., Melamed-Book, N., Hilman, D., Kron, I., and Green, R. M. (2011) Cell autonomous and cell-type specific circadian rhythms in Arabidopsis. *Plant J.* **68**, 520–531
29. Graf, A., Coman, D., Uhrig, R. G., Walsh, S., Flis, A., Stitt, M., and Gruissem, W. (2017) Parallel analysis of arabidopsis circadian clock mutants reveals different scales of transcriptome and proteome regulation. *Open Biol.* **7**
30. Krahmer, J., Hindle, M. M., Martin, S. F., Le Bihan, T., and Millar, A. J. (2015) Sample preparation for phosphoproteomic analysis of circadian time series in Arabidopsis thaliana. *Methods Enzymol* **551**, 405–431
31. Elias, J. E., and Gygi, S. P. (2010) Target-decoy search strategy for mass spectrometry-based proteomics. *Methods Mol. Biol.* **604**, 55–71
32. [preprint] Hindle, M. M., Le Bihan, T., Krahmer, J., Martin, S. F., Noordally, Z. B., Simpson, T. I., and Millar, A. J. (2016) qpMerge: Merging different peptide isoforms using a motif centric strategy. *bioRxiv*. https://doi.org/10.1101/047100
33. Baerenfaller, K., Hirsch-Hoffmann, M., Svozil, J., Hull, R., Russenberger, D., Bischof, S., Lu, Q., Gruissem, W., and Baginsky, S. (2011) pep2pro: a new tool for comprehensive proteome data analysis to reveal information about organ-specific proteomes in Arabidopsis thaliana. *Integr. Biol. (Camb).* **3**, 225–237
34. Vizcaíno, J., Deutsch, E., and Wang, R. (2014) ProteomeXchange provides globally coordinated proteomics data submission and dissemination. *Nat. Biotechnol.* **32**, 223–226
35. Suzuki, R., and Shimodaira, H. (2015) *pvclust: Hierarchical clustering with P-values via multiscale bootstrap resampling*
36. Hughes, M. E., Hogenesch, J. B., and Kornacker, K. (2010) JTK_CYCLE: An efficient nonparametric algorithm for detecting rhythmic components in genome-scale data sets. *J. Biol. Rhythms* **25**, 372–380
37. Benjamini, Y., and Hochberg, Y. (1995) Controlling the false discovery rate: A practical and powerful approach to multiple testing. *J. R. Stat. Soc. B* **57**, 289–300
38. Xue, Y., Ren, J., Gao, X., Jin, C., Wen, L., and Yao, X. (2008) GPS 2.0, a tool to predict kinase-specific phosphorylation sites in hierarchy. *Mol. Cell Proteomics* **7**, 1598–1608
39. Alexa, A., Rahnenführer, J., and Lengauer, T. (2006) Improved scoring of functional groups from gene expression data by decorrelating GO graph structure. *Bioinformatics* **22**, 1600–1607
40. Kalt-Torres, W., Kerr, P. S., Usuda, H., and Huber, S. C. (1987) Diurnal changes in maize leaf photosynthesis: I. Carbon exchange rate, assimilate export rate, and enzyme activities. *Plant Physiol.* **83**, 283–288
41. Van Schaftingen, E., Lederer, B., Bartrons, R., and Hers, H. G. (1982) A kinetic study of pyrophosphate: fructose-6-phosphate phosphotransferase from potato tubers. Application to a microassay of fructose 2,6-bisphosphate. *Eur. J. Biochem.* **129**, 191–195
42. Villadsen, D., and Nielsen, T. H. (2001) N-terminal truncation affects the kinetics and structure of fructose-6-phosphate 2-kinase/fructose-2,6-bisphosphatase from Arabidopsis thaliana. *Biochem. J.* **359**, 591–597
43. [preprint] Noordally, Z. B., Hindle, M. M., Martin, S. F., Seaton, D. D., Simpson, T. I., Bihan, T. L., and Millar, A. J. (2018) Circadian protein regulation in the green lineage I. A phospho-dawn anticipates light onset before proteins peak in daytime. *bioRxiv*. https://doi.org/10.1101/287862
44. Hrabak, E. M., Chan, C. W., Gribskov, M., Harper, J. F., Choi, J. H., Halford, N., Kudla, J., Luan, S., Nimmo, H. G., Sussman, M. R., Thomas, M., Walker-Simmons, K., Zhu, J. K., and Harmon, A. C. (2003) The arabidopsis CDPK-SnRK superfamily of protein kinases. *Plant Physiol.* **132**, 666–680
45. Wang, Y., Liu, Z., Cheng, H., Gao, T., Pan, Z., Yang, Q., Guo, A., and Xue, Y. (2014) EKPD: A hierarchical database of eukaryotic protein kinases and protein phosphatases. *Nucleic Acids Res.* **42**, D496–D502
46. Cho, H. Y., Wen, T. N., Wang, Y. T., and Shih, M. C. (2016) Quantitative phosphoproteomics of protein kinase SnRK1 regulated protein phosphorylation in Arabidopsis under submergence. *J. Exp. Bot.* **67**, 2745–2760
47. Nukarinen, E., Nägele, T., Pedrotti, L., Wurzinger, B., Mair, A., Landgraf, R., Börnke, F., Hanson, J., Teige, M., Baena-Gonzalez, E., Dröge-Laser, W., and Weckwerth, W. (2016) Quantitative phosphoproteomics reveals the role of the AMPK plant ortholog SnRK1 as a metabolic master regulator under energy deprivation. *Sci. Rep.* **6**, 31697
48. Sugden, C., Donaghy, P. G., Halford, N. G., and Hardie, D. G. (1999) Two SNF1-related protein kinases from spinach leaf phosphorylate and inactivate 3-hydroxy-3-methylglutaryl-coenzyme A reductase, nitrate reductase, and sucrose phosphate synthase *in vitro*. *Plant Physiol.* **120**, 257–274
49. Jamsheer K, M., and Laxmi, A. (2015) Expression of Arabidopsis FCS-like Zinc finger genes is differentially regulated by sugars, cellular energy level, and abiotic stress. *Front. Plant Sci.* **6**, 746
50. Jamsheer K, M., Shukla, B. N., Jindal, S., Gopan, N., Mannully, C. T., and Laxmi, A. (2018) The FCS-like zinc finger scaffold of the kinase SnRK1 is formed by the coordinated actions of the FLZ domain and intrinsically disordered regions. *J. Biol. Chem.* **293**, 13134–13150
51. Covington, M. F., Maloof, J. N., Straume, M., Kay, S. A., and Harmer, S. L. (2008) Global transcriptome analysis reveals circadian regulation of key pathways in plant growth and development. *Genome Biol.* **9**, R130
52. Liu, X., Zhu, Y., Zhai, H., Cai, H., Ji, W., Luo, X., Li, J., and Bai, X. (2012) AtPP2CG1, a protein phosphatase 2C, positively regulates salt tolerance of Arabidopsis in abscisic acid-dependent manner. *Biochem. Biophys. Res. Commun.* **422**, 710–715
53. Sahoo, S. A., Raghuvanshi, R., Srivastava, A. K., and Suprasanna, P. (2020) Phosphatases: the critical regulator of abiotic stress tolerance in plants. In: Pandey, G. K., ed. *Protein Phosphatases and Stress Management in Plants*, Springer International Publishing: 163–201
54. Yu, L. P., Miller, A. K., and Clark, S. E. (2003) POLTERGEIST encodes a protein phosphatase 2C that regulates CLAVATA pathways controlling stem cell identity at Arabidopsis shoot and flower meristems. *Curr. Biol.* **13**, 179–188
55. Holtorf, S., Apel, K., and Bohlmann, H. (1995) Comparison of different constitutive and inducible promoters for the overexpression of transgenes in Arabidopsis thaliana. *Plant Mol. Biol.* **29**, 637–646
56. Donahue, J. L., Alford, S. R., Torabinejad, J., Kerwin, R. E., Nourbakhsh, A., Ray, W. K., Hernick, M., Huang, X., Lyons, B. M., Hein, P. P., and Gillaspy, G. E. (2010) The Arabidopsis thaliana myo-inositol 1-phosphate synthase1 gene is required for myo-inositol synthesis and suppression of cell death. *Plant Cell* **22**, 888–903
57. Ma, L., Tian, T., Lin, R., Deng, X. W., Wang, H., and Li, G. (2016) Arabidopsis FHY3 and FAR1 regulate light-induced myo-inositol biosynthesis and oxidative stress responses by transcriptional activation of MIPS1. *Mol. Plant* **9**, 541–557
58. Edwards, K. D., Anderson, P. E., Hall, A., Salathia, N. S., Locke, J. C., Lynn, J. R., Straume, M., Smith, J. Q., and Millar, A. J. (2006) FLOWERING LOCUS C mediates natural variation in the high-temperature response of the arabidopsis circadian clock. *Plant Cell* **18**, 639–650
59. Covington, M. F., and Harmer, S. L. (2007) The circadian clock regulates auxin signaling and responses in arabidopsis. *PLoS Biol.* **5**, 1773–1784
60. Monroe, J. D. (2020) Involvement of five catalytically active Arabidopsis β-amylases in leaf starch metabolism and plant growth. *Plant Direct* **4**, e00199
61. Graf, A., Schlereth, A., Stitt, M., and Smith, A. M. (2010) Circadian control of carbohydrate availability for growth in Arabidopsis plants at night. *Proc. Natl. Acad. Sci. U. S. A.* **107**, 9458–9463
62. Smith, S. M., Fulton, D. C., Chia, T., Thorneycroft, D., Chapple, A., Dunstan, H., Hylton, C., Zeeman, S. C., and Smith, A. M. (2004) Diurnal changes in the transcriptome encoding enzymes of starch metabolism

provide evidence for both transcriptional and posttranscriptional regulation of starch metabolism in arabidopsis leaves. *Plant Physiol.* **136**, 2687–2699
63. Bläsing, O. E., Gibon, Y., Günther, M., Höhne, M., Morcuende, R., Osuna, D., Thimm, O., Usadel, B., Scheible, W. R., and Stitt, M. (2005) Sugars and circadian regulation make major contributions to the global regulation of diurnal gene expression in Arabidopsis. *Plant Cell* **17**, 3257–3281
64. Coruzzi, G. M. (2003) Primary N-assimilation into amino acids in arabidopsis. *Arab. B.* **2**, e0010
65. Wong, H. K., Chan, H. K., Coruzzi, G. M., and Lam, H. M. (2004) Correlation of ASN2 gene expression with ammonium metabolism in arabidopsis. *Plant Physiol.* **134**, 332–338
66. Curran, A., Chang, I. F., Chang, C. L., Garg, S., Miguel, R. M., Barron, Y. D., Li, Y., Romanowsky, S., Cushman, J. C., Gribskov, M., Harmon, A. C., and Harper, J. F. (2011) Calcium-dependent protein kinases from arabidopsis show substrate specificity differences in an analysis of 103 substrates. *Front. Plant Sci.* **2**, 36
67. Kline, K. G., Barrett-Wilt, G. A., and Sussman, M. R. (2010) In planta changes in protein phosphorylation induced by the plant hormone abscisic acid. *Proc. Natl. Acad. Sci. U. S. A.* **107**, 15986–15991
68. Pou, A., Jeanguenin, L., Milhiet, T., Batoko, H., Chaumont, F., and Hachez, C. (2016) Salinity-mediated transcriptional and post-translational regulation of the Arabidopsis aquaporin PIP2;7. *Plant Mol. Biol.* **92**, 731–744
69. Prado, K., Cotelle, V., Li, G., Bellati, J., Tang, N., Tournaire-Roux, C., Martinière, A., Santoni, V., and Maurel, C. (2019) Oscillating aquaporin phosphorylation and 14-3-3 proteins mediate the circadian regulation of leaf hydraulics. *Plant Cell* **31**, 417–429
70. Chen, L. Q., Qu, X. Q., Hou, B. H., Sosso, D., Osorio, S., Fernie, A. R., and Frommer, W. B. (2012) Sucrose efflux mediated by SWEET proteins as a key step for phloem transport. *Science* **335**, 207–211
71. Deyholos, M. K., Cavaness, G. F., Hall, B., King, E., Punwani, J., Van Norman, J., and Sieburth, L. E. (2003) VARICOSE, a WD-domain protein, is required for leaf blade development. *Development* **130**, 6577–6588
72. Kawa, D., Meyer, A. J., Dekker, H. L., Abd-El-Haliem, A. M., Gevaert, K., Van De Slijke, E., Maszkowska, J., Bucholc, M., Dobrowolska, G., De Jaeger, G., Schuurink, R. C., Haring, M. A., and Testerink, C. (2020) SnRK2 protein kinases and mRNA decapping machinery control root development and response to salt. *Plant Physiol.* **182**, 361–377
73. Nielsen, T. H., Rung, J. H., and Villadsen, D. (2004) Fructose-2,6-bisphosphate: A traffic signal in plant metabolism. *Trends Plant Sci.* **9**, 556–563
74. McCormick, A. J., and Kruger, N. J. (2015) Lack of fructose 2,6-bisphosphate compromises photosynthesis and growth in Arabidopsis in fluctuating environments. *Plant J.* **81**, 670–683
75. Villadsen, D., Rung, J. H., Draborg, H., and Nielsen, T. H. (2000) Structure and heterologous expression of a gene encoding fructose-6-phosphate, 2-kinase/fructose-2,6-bisphosphatase from Arabidopsis thaliana. *Biochim. Biophys. Acta* **1492**, 406–413
76. Kulma, A., Villadsen, D., Campbell, D. G., Meek, S. E., Harthill, J. E., Nielsen, T. H., and MacKintosh, C. (2004) Phosphorylation and 14-3-3 binding of Arabidopsis 6-phosphofructo-2-kinase/fructose-2,6-bisphosphatase. *Plant J.* **37**, 654–667
77. Bläsing, O. E., Gibon, Y., Günther, M., Höhne, M., Morcuende, R., Osuna, D., Thimm, O., Usadel, B., Scheible, W. R., and Stitt, M. (2005) Sugars and circadian regulation make major contributions to the global regulation of diurnal gene expression in arabidopsis. *Plant Cell* **17**, 3257–3281
78. Sugano, S., Andronis, C., Ong, M. S., Green, R. M., and Tobin, E. M. (1999) The protein kinase CK2 is involved in regulation of circadian rhythms in Arabidopsis. *Proc. Natl. Acad. Sci. U. S. A.* **96**, 12362–12366
79. Akashi, M., and Nishida, E. (2000) Involvement of the MAP kinase cascade in resetting of the mammalian circadian clock. *Genes Dev.* **14**, 645–649
80. Iitaka, C., Miyazaki, K., Akaike, T., and Ishida, N. (2005) A role for glycogen synthase kinase-3beta in the mammalian circadian clock. *J. Biol. Chem.* **280**, 29397–29402
81. Besing, R. C., Paul, J. R., Hablitz, L. M., Rogers, C. O., Johnson, R. L., Young, M. E., and Gamble, K. L. (2015) Circadian rhythmicity of active GSK3 isoforms modulates molecular clock gene rhythms in the suprachiasmatic nucleus. *J. Biol. Rhythms* **30**, 155–160
82. Martinek, S., Inonog, S., Manoukian, A. S., and Young, M. W. (2001) A role for the segment polarity gene shaggy/GSK-3 in the Drosophila circadian clock. *Cell* **105**, 769–779
83. Nietzsche, M., Schießl, I., and Börnke, F. (2014) The complex becomes more complex: Protein-protein interactions of SnRK1 with DUF581 family proteins provide a framework for cell- and stimulus type-specific SnRK1 signaling in plants. *Front. Plant Sci.* **5**, 54
84. Shin, J., Sánchez-Villarreal, A., Davis, A. M., Du, S.-x., Berendzen, K. W., Koncz, C., Ding, Z., Li, C., and Davis, S. J. (2017) The metabolic sensor AKIN10 modulates the Arabidopsis circadian clock in a light-dependent manner. *Plant Cell Environ.* **40**, 997–1008
85. Sánchez-Villarreal, A., Davis, A. M., and Davis, S. J. (2018) AKIN10 activity as a cellular link between metabolism and circadian-clock entrainment in Arabidopsis thaliana. *Plant Signal. Behav.* **13**, e1411448
86. Frank, A., Matiolli, C. C., Viana, A. J. C., Hearn, T. J., Kusakina, J., Belbin, F. E., Wells Newman, D., Yochikawa, A., Cano-Ramirez, D. L., Chembath, A., Cragg-Barber, K., Haydon, M. J., Hotta, C. T., Vincentz, M., Webb, A. A. R., *et al*. (2018) Circadian entrainment in arabidopsis by the sugar-responsive transcription factor bZIP63. *Curr. Biol.* **28**, 2597–2606.e6
87. González, A., Hall, M. N., Lin, S. C., and Hardie, D. G. (2020) AMPK and TOR: The Yin and Yang of cellular nutrient sensing and growth control. *Cell Metab.* **31**, 472–492
88. Larkin, M. A., Blackshields, G., Brown, N. P., Chenna, R., McGettigan, P. A., McWilliam, H., Valentin, F., Wallace, I. M., Wilm, A., Lopez, R., Thompson, J. D., Gibson, T. J., and Higgins, D. G. (2007) Clustal W and Clustal X version 2.0. *Bioinformatics* **23**, 2947–2948
89. Waterhouse, A. M., Procter, J. B., Martin, D. M., Clamp, M., and Barton, G. J. (2009) Jalview Version 2-A multiple sequence alignment editor and analysis workbench. *Bioinformatics* **25**, 1189–1191
90. O'Shea, J. P., Chou, M. F., Quader, S. A., Ryan, J. K., Church, G. M., and Schwartz, D. (2013) pLogo: a probabilistic approach to visualizing sequence motifs. *Nat. Methods* **10**, 1211–1212